

**DOKUZ EYLÜL UNIVERSITY
GRADUATE SCHOOL OF NATURAL AND APPLIED
SCIENCES**

**THE IMMOBILIZATION OF COPPER (II)
ACETYLACETONATE COMPLEX ONTO SOLID
SUPPORTS AND THEIR CHARACTERIZATION**

Senem COŞKUN

**August, 2010
İZMİR**

**THE IMMOBILIZATION OF COPPER (II)
ACETYLACETONATE COMPLEX ONTO SOLID
SUPPORTS AND THEIR CHARACTERIZATION**

**A Thesis Submitted to the
Graduate School of Natural and Applied Sciences of Dokuz Eylül University
In Partial Fulfillment of the Requirements for the Degree of Master of Science
in
Chemistry**

**by
Senem COŞKUN**

**August, 2010
İZMİR**

MSc THESIS EXAMINATION RESULT FORM

We have read the thesis entitled “**THE IMMOBILIZATION OF COPPER (II) ACETYLACETONATE COMPLEX ONTO SOLID SUPPORTS AND THEIR CHARACTERIZATION**” completed by **SENEM COŞKUN** under supervision of **PROF. DR. MÜRÜVVET YURDAKOÇ** and we certify that in our opinion it is fully adequate, in scope and in quality, as a thesis for the degree of Master of Science in Chemistry.

.....
Prof. Dr. Mürüvvet YURDAKOÇ

Supervisor

.....

Jury Member

.....

Jury Member

Prof. Dr. MUSTAFA SABUNCU
Director

Graduate School of Natural and Applied Sciences

ACKNOWLEDGMENTS

I would like to express my gratitude to my research, to my research advisor Prof. Dr. Mürüvvet YURDAKOÇ, whose expertise, encouragement, understanding, support, advice, guidance and patience, added considerably to my thesis study.

I would like to thank Prof. Dr. Kadir YURDAKOÇ for his studies, guidance, supports and useful comments on the preparation of the thesis and his geniality.

I would also like to thank my mother and my sister for the support they provided me through my entire life and in particular.

Senem COŞKUN

THE IMMOBILIZATION OF COPPER (II) ACETYLACETONATE COMPLEX ONTO SOLID SUPPORTS AND THEIR CHARACTERIZATION

ABSTRACT

In accordance with the green chemistry principles, the immobilization of transition metal complexes with catalytic properties onto solid matrixes or organic polymers is an important research subject that has received much attention in recent years.

Clay minerals occur abundantly in nature and their high surface area, sorptive and ion-exchange properties have been exploited for catalytic applications through decades. Clays, in general, are important and useful low-cost materials with a wide range of applications, namely in industry, engineering, agriculture, pharmaceuticals, absorbents, surface coatings, and ceramics, and for environment purposes.

Bentonite is a 2:1 sheet rock with one octahedral and two silica sheets, which form a layer. Layers are held together by van der Waals forces. It is used as industrial raw materials in many applications. The major uses are iron pelletizing, pet adsorbents, drilling fluids, bleaching of edible oils, applications in civil engineering and the foundry industry. Because of these properties of Bentonite for the removal of heavy metal waste is the most promising type of clay is considered. On the other hand, Siral compounds are synthetic silica-aluminas while Bentonite is a natural product. Siral 80 composed of about the same percentages of silica and alumina as in Bentonite which can be both used as catalysts themselves and also support materials in the area of heterogeneous catalysis.

In this study, natural Bentonite from Enez/Edirne as a clay and Siral 80 were used as solid supports for the immobilization. The basic difference between these materials is former natural material; latter is synthetic silica-alumina. As active components, copper (II) acetyl acetate was used in the preparation procedure. Two types of method were applied in the preparation of heterogeneous catalysts.

The prepared catalysts samples were characterized with several methods, such as X-Ray Fluorescence (XRF), Thermogravimetric Analyses (TGA/DTG), X-Ray Powder Diffraction (XRD), Scanning Electron Microscope (SEM), Atomic Absorption Spectroscopic (AAS), Fourier Transform Infrared (FTIR) and Specific Surface Area Determination (BET) were also be determined.

Keywords: (3-aminopropyl)triethoxysilane, Bentonite, Siral, APTES, Copper (II) acetylacetonate

BAKIR (II) ASETİLASETONAT KOMPLEKSİNİN KATI DESTEK MADDELERİ ÜZERİNE AKTARIMI VE KARAKTERİZASYONU

ÖZ

Çevre dostu kimya (:Green Chemistry) kapsamında özellikle son yıllarda katalitik özellikleri olan geçiş metallere katı ya da polimer taşıyıcı malzeme üzerine aktarımı yoluyla katalizörlerin hazırlanmaları ve sanayide çeşitli kimyasal tepkimelerde katalizör olarak kullanılmaları yaygınlaşmıştır.

Doğal ya da işlenmiş killer, ucuz olmaları ve bollukları nedeniyle kimya sanayii, ziraat, yüzey kaplama ve çevre amaçlı olarak kullanıldıkları gibi aynı zamanda doğrudan katalizör ya da katalizör taşıyıcısı olarak kullanılırlar. Killere adsorbent olarak bunun yanı sıra mühendislik, tarım, ilaç, yüzey kaplama, seramik ve çevre gibi geniş kullanım alanına sahip, düşük maliyetli materyallerdir.

Bentonit, 2:1 katman formunda bir sekizyüzlü ve iki silis yaprak formundadır. Katmanlar birbirine van der Waals bağlarıyla bağlanmış şekildedir. Bu çeşit yapılar katyon değişim özelliği ve şişme kabiliyetleri gösterirler. Bentonitin fiziksel ve kimyasal özelliklerinden bazıları; geniş özgül yüzey alanı, katyon değişim kapasitesi ve organik, inorganik iyonlarının adsorpsiyon kabiliyetlerine sahip olmasıdır. Bu özelliklerinden dolayı Bentonit ağır metal atıklarının uzaklaştırılması için en umut verici kil çeşidi olarak kabul edilir.

Bentonit doğal bir kil olmasına rağmen Sıral bileşikler, sentetik silika aluminadır. Silika ve aluminanın değişik oranlarda karıştırılmalarıyla hazırlanırlar, özellikle petrokimya sanayiinde heterojen katalizör ve katalizör taşıyıcısı olarak kullanılırlar.

Bu çalışmada kil olarak doğal Enez/Edirne Bentoniti ve Sıral 80 kullanılmıştır. Bu iki madde arasındaki temel fark, kilin doğal madde, Sıral 80'in ise sentetik silika-alumina bileşiği olmasıdır. Aktif bileşen olarak bakır asetil asetonat kullanılmıştır.

Çalıřmada iki farklı hazırlama yöntemi uygulanarak heterojen katalizörler hazırlanmıřtır.

Hazırlanan katalizörler X-Ray Floresans (XRF), Thermogravimetrik Analiz (TGA/DTG), X-Iřını Toz Kırınımı (XRD), Taramalı Electron Mikroskop (SEM), Atomic Absorption Spectroskopi (AAS), Özgöl Yüzey Alanı (BET) and Fourier Transform Infrared (FTIR) yöntemleriyle karakterize edilmiřtir.

Anahtar sözcükler: (3-aminopropil)trioksisilan, Bentonit, Sıral, APTES, Bakır (II) asetilasetonat

CONTENTS

	Page
MSc THESIS EXAMINATION RESULT FORM.....	ii
ACKNOWLEDGEMENTS	iii
ABSTRACT.....	iv
ÖZ	vi
CHAPTER ONE- INTRODUCTION	1
1.1 Clays onto General Information.....	1
1.1.1 Definitions and classifications	1
1.1.2 Structure of clay minerals	1
1.2 Montmorillonites.....	7
1.3 Properties of clays	9
1.3.1 Ion exchange.....	9
1.3.2 Swelling	9
1.3.3 Intercalation and cation-exchange.....	9
1.4 Pillared Clay.....	10
1.5 Bentonite	11
1.5.1 Use of Bentonite	13
1.6 Siral Compounds.....	14
1.7 (3-aminopropyl)triethoxysilane (APTES).....	15
1.8 Metal acetylacetonates	15
1.8.1 Copper (II) acetylacetonate	16
1.9 The purpose of the study	16

CHAPTER TWO- EXPERIMENTAL STUDIES	18
2.1 Materials, reagents and solvents	18
2.2 Preparation of clay samples	18
2.2.1 Functionalisation of the clay with (3-aminopropyl)triethoxysilane	18
2.2.2 Anchoring of copper (II) acetylacetonate onto APTES functionalized clay	18
2.2.3 Direct anchoring of copper (II) acetylacetonate onto clay	19
2.3 Characterization of Clay Sample	20
2.3.1 X-Ray Fluorescence (XRF) Analysis	20
2.3.2 B.E.T Specific Surface Area Determination	20
2.3.3 Atomic Absorption Spectroscopic (AAS) Analysis	20
2.3.4 X-Ray Powder Diffraction (XRD) Analysis	21
2.3.5 Thermogravimetric Analyses (TGA/DTG)	21
2.3.6 Fourier Transform Infrared (FTIR) Analysis	21
2.3.7 Scanning Electron Microscope (SEM) Analysis	21
 CHAPTER THREE- RESULTS.....	 22
3.1 Results	22
3.1.1 X-Ray Fluorescence (XRF) Results	22
3.1.2 Cu (II) the determination with Atomic Absorption Spectroscopy Results ...	23
3.1.3 B.E.T Analyses Results.....	24
3.1.4 Fourier Transform Infrared (FTIR) Results	25
3.1.5 X-ray Diffractograms (XRD) Results	32
3.1.6 Thermogravimetric Analyses (TGA/DTG) Results	34
3.1.7 Scanning Electron Microscope (SEM) Results.....	39
 CHAPTER FOUR- DISCUSSION	 44
4.1 Discussion	44
 REFERENCES	 47

CHAPTER ONE

INTRODUCTION

1.1 Clays on to General Information

Clays have been used since the beginning of civilization and they still keep their position among the most important industrial raw materials.

1.1.1 Definitions and Classification

During the last decade, the engineering of porosity in common materials such as silica, zeolites and clays is emerging as an area of great scientific and technological interest (Ahenach et al., 2000). Clay minerals occur abundantly in nature and their high surface area, sorptive and ion-exchange properties have been exploited for catalytic applications through decades (Rajender et al., 2002). Materials with tunable pores become particularly important towards applications in the field of adsorption and catalysis (Ahenach et al., 2000).

1.1.2 Structure of Clay Minerals

The term clay can be defined in several ways. Clay can refer to all soil particles less than a given size, usually 2 μm . In soils, this particle size range is composed of clay minerals and other components. Clay minerals give a clay soil its plastic and cohesive properties. Other components of the clay size fraction include nonclay minerals (e.g., marl and chalk), amorphous material, and organic material.

Clay minerals are made up of layered silicates. Chemical properties of the surfaces of silicates and, in particular, clay minerals are strongly dependent on their mineral structure. They are crystalline materials of very fine particle size ranging from 150 to less than 1 micron (colloidal form). There are two basic building blocks viz. tetrahedral and octahedral layers, which are common to clay minerals. The basic

unit of montmorillonite crystals is an extended layer composed of an octahedral alumina sheet (O) between two tetrahedral silica sheets (T), forming a TOT unit. The stacks of TOT layers produce the montmorillonite crystals. Tetrahedral layers consist of continuous sheets of silica tetrahedra linked via three corners to form a hexagonal mesh and the fourth corner of each tetrahedron (normal to the plane of the sheet) is shared with octahedra in adjacent layers. Octahedral layers in clay mineral, on the other hand, consist of flat layers of edge-sharing octahedra, each formally containing cations at its centre (usually Mg^{2+} or Al^{3+}) and OH^- or O^{2-} at its apices. Octahedral layers may be trioctahedral or dioctahedral depending on the degree of occupancy of the octahedral sites. These different classes of clay minerals, namely the 1:1, 2:1, etc. have a different arrangement of tetrahedral and octahedral layers. Structural units of clays therefore consist of either;

- (a) alternating tetrahedral or octahedral sheets (OT or 1:1 structure), e.g. kaolinite group,
- (b) a sandwich of one octahedral sheet between two tetrahedral sheets (TOT or 2:1 structure), e.g. smectite clay minerals of which the most common member is montmorillonite,
- (c) an arrangement in which the three layer TOT units alternate with a brucite layer (2:1:1 structure), e.g. chlorite.

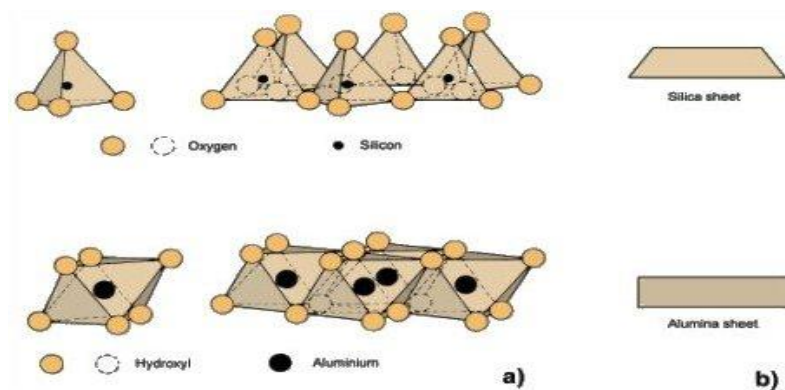


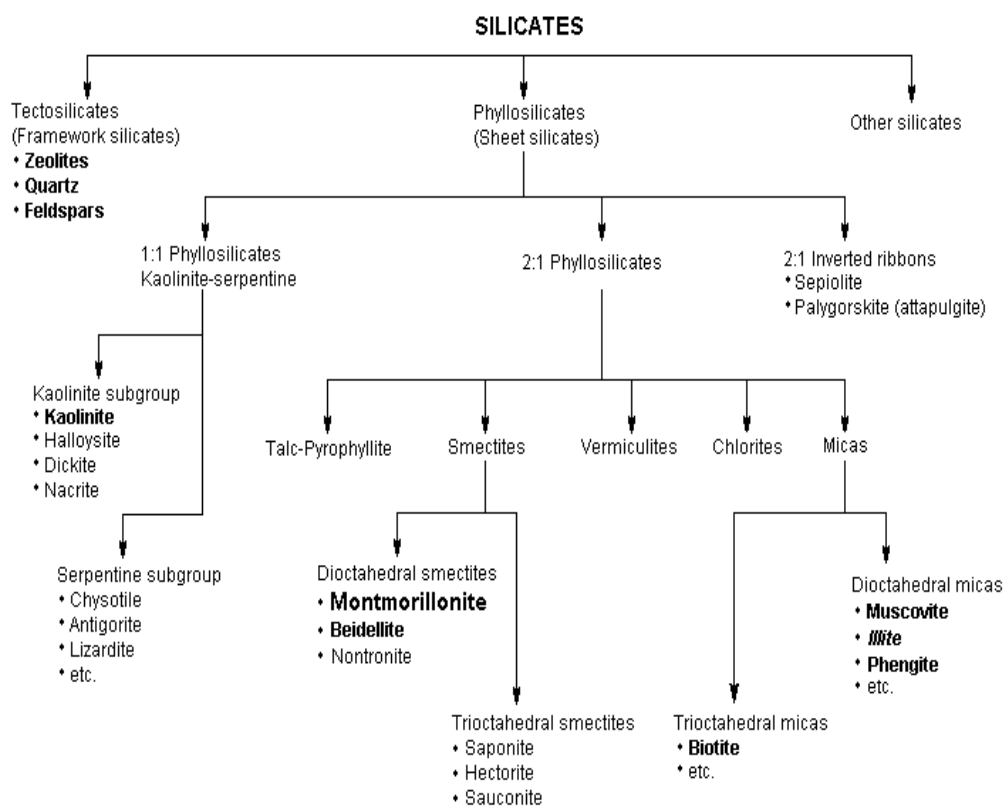
Figure 1.1 Basic units of clay minerals and the silica and alumina sheets

Tetrahedral sites in clay minerals are mainly occupied by Si^{4+} . However, isomorphous substitution by Al^{3+} is also common. In the case of trioctahedral, octahedral sites are generally occupied by Mg^{2+} . Isomorphous substitution by other divalent cations such as Fe^{2+} or Ni^{2+} or by univalent cations such as Li^+ is common. In the case of dioctahedral clay minerals, octahedral sites are predominantly occupied by Al^{3+} and isomorphous substitution by other trivalent cations like Fe^{3+} , Cr^{3+} or divalent cations like Mg^{2+} or Fe^{2+} are common in 2:1 structures (Rajender et al., 2002).

These cations are exchangeable due to their loose binding and, together with broken bonds (approximately 20% of exchange capacity), give montmorillonite a rather high (about 100 meq/100 g) cation exchange capacity, which is little affected by particle size. This cation exchange capacity allows the mineral to bind not only inorganic cations such as cesium but also organic cations such as the herbicides diquat, paraquat (Weber et al., 1965), and s-triazines (Weber et al., 1970), and even bio-organic particles such as (Lipson & Stotzky, 1983) rhinoviruses and proteins (Potter & Stollerman, 1961), which appear to act as cations. Variation in exchangeable cations affects the maximum amount of water uptake and swelling. These are greatest with sodium and least with potassium and magnesium.

Isomorphous substitutions in the octahedral sheet (few tetrahedral substitutions are observed in montmorillonite) create an excess of negative structural charge that is delocalized in the lattice. Cations located between two consecutive layers contribute to compensate the structural charge and to keep the layers bound. These cations can easily be exchanged, since they are retained by electrostatic attractions (Stumm, 1997). The surface area associated with the basal surfaces of the extended TOT units is known as the interlayer surface when it corresponds to consecutive layers or as the external surface when it corresponds to the external basal surfaces of a crystal.

Table 1.1 Classification of silicates



Minerals that can be frequently found in Bentonite or kaolin are in bold; the main components are in large typeface. Illite is a component of common soil and sediments and is classified as a mica (Bailey, 1980, Rieder et al., 1998).

Clays have been used since the beginning of civilization and they still keep their position among the most important industrial raw materials. There are three basic classes of clays: smectites, kaolinite and micas (Orolinova et al., 2009).

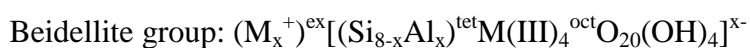
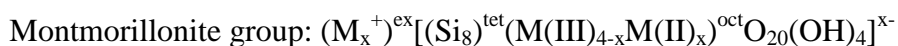
The basic crystal structure of smectite clays have a sandwich structure and their negatively charged aluminaosilicate layers are separated by positively charged cations such as sodium or calcium cations. Atoms in these sheets common to both layers are oxygens. These three-layer units are stacked one above another with oxygens in neighbouring layers adjacent to each other. This produces a weak bond, allowing water and other polar molecules to enter between layers and induce an

expansion of the mineral structure. When large organic and inorganic cations separate the clay sheets, sufficient interlamellar space is created to allow a variety of uses such as adsorbents and catalysts (Zhou et al., 2004). Smectite group minerals of clay minerals has a dioctahedral or trioctahedral 2:1 layer structure, with isomorphous substitution that leads to a negative layer charge of less than 1.2 per formula unit. Differences in the substitutions within the lattice in terms of position and elemental composition give rise to the various montmorillonite clay minerals: montmorillonite, nontronite, saponite, hectorite, sauconite, beidellite, volkhonskoite, pimelite, and griffithite.

Smectites are divided into four subclasses depending upon;

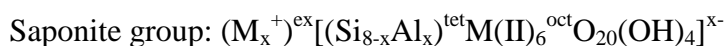
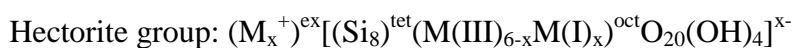
- (a) the type of octahedral layer (dioctahedral or trioctahedral),
- (b) the predominant location of layer charge sites (octahedral or tetrahedral).

Montmorillonite and beidellite groups shown below are dioctahedral smectites with layer charges predominantly in octahedral and tetrahedral sites, respectively.



where M^+ is the exchangeable cation present in the interlayer (e.g. Na^+) and $M(III)$ and $M(II)$ are non-exchangeable octahedrally coordinated trivalent and divalent cations (e.g. Al^{3+} and Mg^{2+}), respectively and the layer charge is $0.5 < x < 1.2$.

Hectorite and saponite groups are trioctahedral smectites with layer charges predominantly in octahedral and tetrahedral sites, respectively. Their ideal formulae are;



M(II) and M(I) are non-exchangeable octahedrally coordinated divalent and univalent cations (e.g. Mg^{2+} and Li^+), respectively and the layer charge is $0.5 < x < 1.2$.

The name "kaolin" is derived from the word Kau-Ling, or high ridge, the name given to a hill near Jau-chau Fu, China, where kaolin was first mined (Sepulveda et al., 1983). Kaolin is clay that contains 10–95% of the mineral kaolinite and usually consists mainly of kaolinite (85–95%). The structure of kaolinite is a tetrahedral silica sheet alternating with an octahedral alumina sheet. These sheets are arranged so that the tips of the silica tetrahedrons and the adjacent layers of the octahedral sheet form a common layer (Grim, 1968). In the layer common to the octahedral and tetrahedral groups, two-thirds of the oxygen atoms are shared by the silicon and aluminium, and then they become O^{2-} instead of $-\text{OH}$. The charges within the structural unit are balanced. Analyses of many samples of kaolinite minerals have shown that there is very little substitution in the lattice (Grim, 1968). The molecular formula that is common for the kaolinite group (kaolinite, nacrite, dickite) is $\text{Al}_2\text{Si}_2\text{O}_5(\text{OH})_4$.

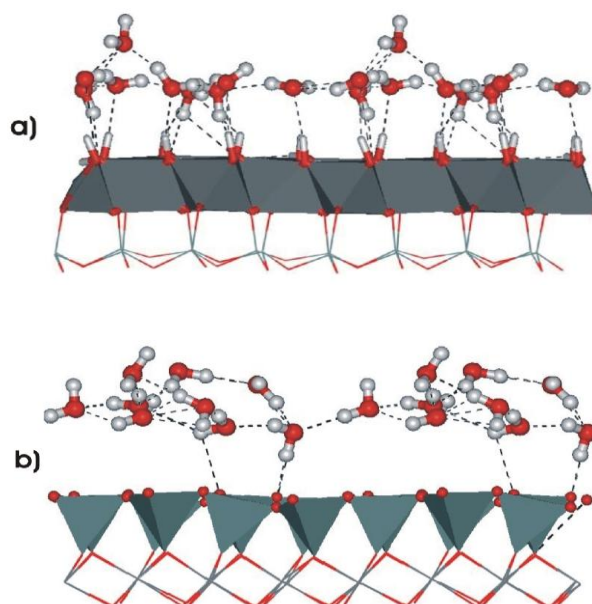


Figure 1.2 Distribution of the monomolecular water layer on the a) octahedral b) tetrahedral surfaces of the kaolinite layer

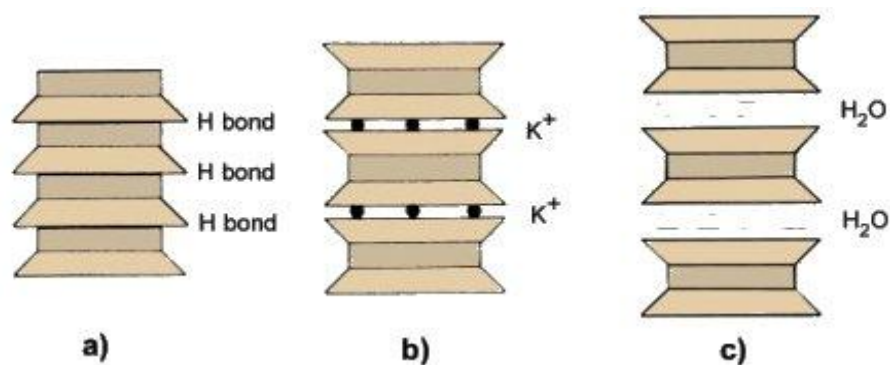


Figure 1.3 Structure of the main clay minerals: a) kaolinite, b) illite c) montmorillonite based on combined sheets

Clays, in general, are important and useful low-cost materials with a wide range of applications, namely in industry, engineering, agriculture, pharmaceuticals, absorbents, surface coatings, and ceramics, and for environment purposes. These materials, either natural or modified, can also be used in catalysis, both as catalysts and catalyst supports. In smectites the variety of applications is related to their unique properties such as high surface area, cation-exchange capacity, and swelling ability (Pereira et al., 2007).

1.2 Montmorillonites

Montmorillonite, a dioctahedral clay with the 2:1 layer linkage, has a high cation-exchange capacity (CEC) ranging from 70 to 130 meq/100 g, most of which is due to the isomorphous substitution of its main cations, Si^{4+} and Al^{3+} within the structure with cations of lower valency, but a lesser amount is due to the charges at the edge of the sheets. The cation substitutions mainly take place in the octahedral sheets and may induce an enormous change in the physicochemical properties of clay minerals (Caglar, 2008).

The periodic structure of the montmorillonite crystals is interrupted at the edges, where the broken bonds compensate their charge by the specific adsorption of protons and water molecules (Schindler & Stumm, 1987; Stumm & Wollast, 1990; Stumm, 1997). This interruption of the periodic structure confers to the edge surface

an amphoteric character — i.e., a pH-dependent surface charge and the capacity to react specifically with cations, anions, and molecules (organic and inorganic), forming chemical bonds. The external and interlayer surface area represents approximately 95% of the total surface area of montmorillonite. The "active" surface area is close to 5% in montmorillonite (Rieder et al., 1998).

Montmorillonite is the most important smectite used in catalytic applications. Good swelling properties allow a wide variety of catalytically active forms of montmorillonite to be prepared (e.g. containing acidic cations, metal complexes, photocatalytically active cations, etc.).

Montmorillonites are most frequently used as Brønsted acid catalysts, where the exchangeable cations are either protons or polarizing cations (e.g. Al^{3+} , Cr^{3+} or Fe^{3+}). Acid site strength depends upon the type of interlayer cations present ($\text{H}_3\text{O}^+ > \text{Al}^{3+} > \text{Ca}^{2+} > \text{Na}^+$). Higher acid strength generally leads to greater catalytic activity, but poorer product selectivity. Controlling the acid site strength by choice of interlayer cations proves to be useful for 'fine-tuning' the catalyst selectivity. Leads to increased surface area and concentration of weak acid sites, but a decrease in concentration of strong acid sites. Acid leached montmorillonite is particularly useful for catalytic applications requiring only weak acid sites, where strong acid sites give rise to poor selectivity (Rajender et al., 2002). These properties make various montmorillonites useful as binders, plasticizers, lubricants and rheological control agents (Alemdar et. al., 2005).

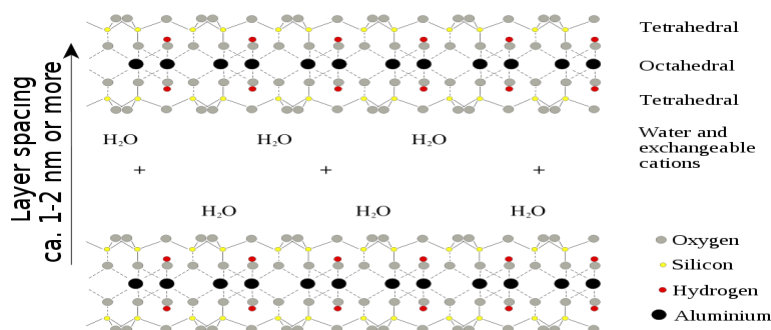


Figure 1.4 Structure of montmorillonite

1.3 Properties of clays

1.3.1 Ion Exchange

Isomorphous substitution of cations in the lattice by lowervalent ions, e.g. the substitution of aluminium for silicon, magnesium and/or ferrous ion for aluminum or sometimes lithium for magnesium, leaves a residual negative charge in the lattice that is balanced by other cations. These can be readily replaced by other cations when brought into contact with these ions in aqueous solution (Alemdar et. al., 2005).

1.3.2 Swelling

Many clay minerals absorb water between their layers, which move apart and the clay swells. For efficient swelling, the energy released by cations and/or layer solvation must be sufficient to overcome the attractive forces (such as hydrogen bonding) between the adjacent layers. In 1:1 (OT) clay minerals (kaolinite), water forms strong hydrogen bonds with hydroxyl groups on hydrophilic octahedral layers, allowing swelling to occur. With 2:1 (TOT) clay minerals, the ability to swell depends on the solvation of interlayer cations and layer charge. Clays with 2:1 structures and low layer charge (e.g. talc and pyrophyllite) have very low concentration of interlayer cations and therefore do not swell readily. At the other extreme, those with very high layer charges (e.g. mica) have strong electrostatic forces holding alternate anionic layers and the interlayer cations together, thus preventing swelling. Those with univalent interlayer cations swell most readily and with divalent, trivalent and polyvalent cations, swelling decreases accordingly (Alemdar et. al., 2005).

1.3.3 Intercalation and Cation-Exchange

In swelling clay minerals, such as smectites, the interlayer cations can undergo exchange with cations from external solutions. The concentration of exchangeable

cations is called CEC, usually measured in milliequivalents per 100 g of dried clay. Since smectites have the highest concentration of interlayer cations, they have the highest cation exchange capacities (typically 70-120 mequiv./100 g). Structural defects at layer edges give rise to additional CEC and a small amount of anion exchange capacity (Alemdar et. al., 2005).

1.4 Pillared Clays

Pillared interlayer clays (or pillared clays, PILCs) are a relatively new class of modified clays. PILCs are typically synthesized by exchanging the interlayer cations with a pillaring agent (large oligomeric polycations) such as the Keggin-like Al_{13} oligomer $[\text{Al}_{13}\text{O}_4(\text{OH})_{24}(\text{H}_2\text{O})_{12}]^{7+}$. Upon calcination, the resulting materials contain metal oxide pillars that prop open the clay sheets and expose the internal surfaces of the clay layers (Zhu et al., 2007).

Between the TOT layers of a smectite, large cationic species (e.g. aluminum chlorhydroxide) can be inserted by cation exchange. Such bulky species act like pillars, propping apart the TOT layers (typically by 0.3-1.5 nm). Slit-shaped pores are formed between pillars and TOT layers, which give rise to a uniform two-dimensional micropore system between adjacent TOT layers. Pore entry sizes are governed by the height of the pillars and the distance between them and can be designed to suit specific application. A wide range of bulky cationic species have been used to prepare pillared smectites, including organic cations (e.g. quaternary ammonium cations and 1,4 diazabicyclo-[2.2.2] octane, DABCO) and inorganic cations (e.g. polyoxyhydroxides of aluminum and zirconium) (Alemdar et. al., 2005).

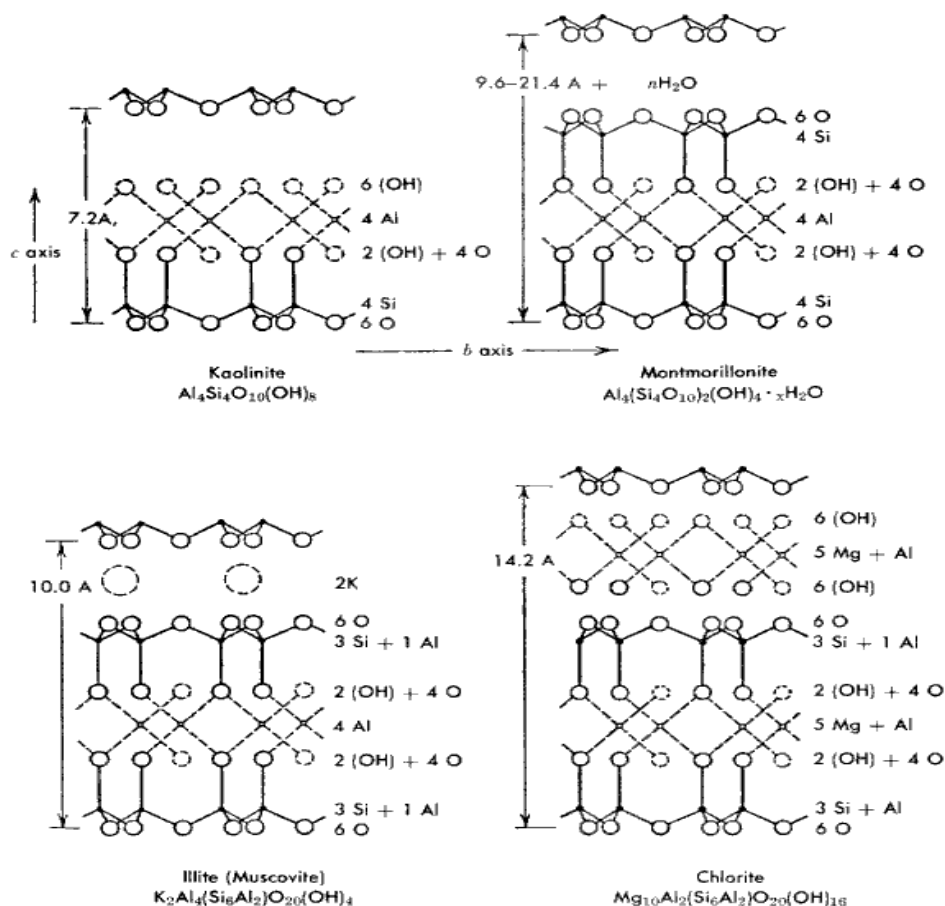


Figure 1.5 Clay layer structures (Anthoni, 2000)

1.5 Bentonite

Bentonite is natural clay that is found in many places of the world (Eren et al., 2008). It is smectite group clay formed from the alteration of siliceous, glass-rich volcanic rocks such as tuffs and ash deposits (Hasmukh et al., 2007). Bentonite is a rock formed of highly colloidal composed mainly of montmorillonite. Any clay of volcanic origin that contains montmorillonite is referred to as Bentonite. It belongs to the 2:1 clay family, the basic structural unit of which is composed of two tetrahedrally coordinated sheets of silicon ions surrounding a sandwiched octahedrally coordinated sheet of aluminum ions. The isomorphous substitution of Al^{3+} for Si^{4+} in the tetrahedral layer and Mg^{2+} or Zn^{2+} for Al^{3+} in the octahedral layer results in a net negative surface charge on the clay (Eren et al., 2008). In this clay

mineral the silicate layers are joined through relatively weak dipolar and van der Waals forces and the cations Na^+ and Ca^{2+} located in the interlayers. Compared with other clay types, it has excellent sorption properties and possesses sorption sites available within its interlayer space as well as on the outer surface and edges (Eren et al., 2008).

Bentonite may contain feldspar, cristobalite, and crystalline quartz. The special properties of Bentonite are an ability to form thixotropic gels with water, an ability to absorb large quantities of water, and a high cation exchange capacity. The properties of Bentonite are derived from the crystal structure of the smectite group, which is an octahedral alumina sheet between two tetrahedral silica sheets. Variations in interstitial water and exchangeable cations in the interlayer space affect the properties of Bentonite and thus the commercial uses of the different types of Bentonite.

Freshly exposed Bentonite is white to pale green or blue and, with exposure, darkens in time to yellow, red, or brown. The special properties of Bentonite are an ability to form thixotropic gels with water, an ability to absorb large quantities of water with an accompanying increase in volume of as much as 12–15 times its dry bulk, and a high cation exchange capacity (Ma L & Tang J, 2002).

Physical characteristics of Bentonite are affected by whether the montmorillonite composing it has water layers of uniform thickness or whether it is a mixture of hydrates with water layers of more than one thickness. Loss of absorbed water from between the silicate sheets takes place at relatively low temperatures (100–200 °C). Loss of structural water (i.e., the hydroxyls) begins at 450–500 °C and is complete at 600–750 °C. Further heating to 800–900 °C disintegrates the crystal lattice and produces a variety of phases, such as mullite, cristobalite, and cordierite, depending on initial composition and structure. The ability of montmorillonite to rapidly take up water and expand is lost after heating to a critical temperature, which ranges from 105 to 390 °C, depending on the composition of the exchangeable cations. The ability to take up water affects the utilization and commercial value of Bentonite (Cirep, 2003)

Adsorption of metal ions onto montmorillonite appears to involve two distinct mechanisms: (I) an ion exchange reaction at permanent charge sites, and (ii) formation of complexes with the surface hydroxyl groups (Eren et al., 2008).

1.5.1 Use of Bentonite

In view of the widespread distribution of Bentonite in nature and its use in an enormous variety of consumer products, general population exposure to low concentrations is ubiquitous.

Major uses of Bentonite include binding foundry sand in moulds; absorbing grease, oil, and animal wastes; pelletizing taconite iron ore; and improving the properties of drilling muds. Speciality uses include serving as an ingredient in ceramics; waterproofing and sealing in civil engineering projects, such as landfill sites and nuclear waste repositories; serving as a filler, stabilizer, or extender in adhesives, paints and as a bonding agent in animal feeds; clarifying wine; and purifying wastewater (Bernstein et al., 1994)

Bentonite is highly valued by its sorption properties, which stem from its high surface area, swelling capacity and cation exchange capacity. Many of them are related to the crystal isomorphic substitution. Some properties of this clay are improved commonly with mineral acid activation, such as surface area, porosity and acid sites. Acid activated Bentonites are widely used in various fields, for example catalysts, catalyst supports in the chemical industry and a component of carbonless copying papers as well as detergent in paper industry (Araujo et al., 2004). In addition, Bentonite includes ceramics, cosmetics, polymer nanocomposites and foundry industry (Zhansheng et al., 2007). It is used in many of industrial areas such as an emulsifier agent for asphaltic and resinous substances, as an adhesive agent in horticultural sprays and insecticides, in concrete mixtures, as a plasticizer in ceramic bodies as a bleaching in vegetable oils and drilling mud (Paluszkiewicz et al., 2008).

Due to its physical and chemical properties, i.e., large specific surface area, cation exchange capacity and adsorptive affinity for organic and inorganic ions, Bentonite is considered one of the most promising candidates for use in decontamination and

disposal of high-level heavy metal wastes (Zuzana et al., 2009). Furthermore Bentonite is used in a wide range of applications such as drilling mud, foundry sand binding, iron-ore pelletizing and civil engineering uses such as waterproofing and sealant (Hasmukh et al., 2007).


1.6 Siral Compounds

Siral compounds are synthetic silica-aluminas now produced by SASOL AG/Germany. Some properties are given below. However, Siral 80 was purchased from Condea AG/Germany as a gift in 1999. (Retrieved: June, 2010 from <http://www.sasoltechdata.com/tds/SIRAL.pdf>).

Table 1.2 Components of Sirals

High Purity Aluminas
SIRAL®

PRODUCT INFORMATION
Silica Aluminas (Alumina phase = Boehmite)



Typical chemical and physical properties		SIRAL 1	SIRAL 5	SIRAL 10	SIRAL 20	SIRAL 28M	SIRAL 30	SIRAL 40
Al ₂ O ₃ + SiO ₂	[%]	75	75	75	75	75	75	75
LOI	[%]	25	25	25	25	25	25	25
Al ₂ O ₃ : SiO ₂	[%]	99:1	95:5	90:10	80:20	72:28	70:30	60:40
C	[%]	0.2	0.2	0.2	0.2	0.2	0.2	0.2
Fe ₂ O ₃	[%]	0.01	0.01	0.01	0.01	0.01	0.01	0.01
Na ₂ O	[%]	0.002	0.005	0.005	0.005	0.01	0.01	0.01
Loose bulk density	[g/l]	600-800	450-650	400-600	300-500	250-450	250-450	250-450
Particle size (d ₉₀)	[µm]	50	50	50	50	50	50	50
Surface area (BET)*	[m ² /g]	280	370	400	420	470	470	500
Pore volume*	[ml/g]	0.50	0.70	0.75	0.75	1.40	0.80	0.90

* After activation at 550°C for 3 hours.

1.7 (3-aminopropyl)triethoxysilane (APTES)

Human or environmental exposure to (3-aminopropyl)triethoxysilane (APTES) (Figure 1.6) is limited to accidental acute exposures. In production, this material is mostly handled in closed systems. Necessary engineering controls during production include proper ventilation, containment, safety equipment and actual hardware designed to minimize exposure through splashing, or exposure to the air. Transfer of this material is in closed pipes rather than in open systems to minimize loss of this material (hydrolysis) although some customers do transfer the material in open systems. APTES is transported from the production site as the parent silane to processors/formulators. After curing the parent silane is consumed into the polymer matrix and no longer exists and greatly reduces potential for consumer or worker exposure.

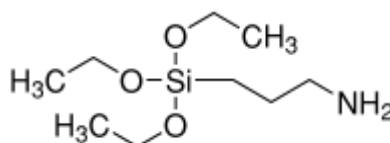


Figure 1.6 Structure of (3-aminopropyl) triethoxysilane (APTES)

Since APTES is sensitive to hydrolysis, which may occur during testing, observed toxicity is likely due to the hydrolysis products ethanol and trisilanols Hernandez O., SIDS Initial Assessment Report For SIAM 17, Arona, Italy, 11-14 November 2003 Retrieved: June, 2010 from <http://www.inchem.org/documents/pdf/>.

1.8 Metal Acetylacetonates

Metal acetylacetonates are used as catalysts for polymerization of olefins and transesterification. They are used as PVC stabilizer. They are used as curing agents for epoxy resins, acrylic adhesives and silicone rubbers. They are used as solvents, lubricant additives, paint drier, and pesticides. They are used in glass coatings.

Acetylacetonone is used in the preparation of metal acetylacetonates for catalyst application. The oxygen atoms in delocalized anion (acetylacetonate) left after the removal of a proton from an enol is readily bound to transition metal ions and form chelate complexes which are freely soluble organic solvents, in contrast to the related metal halides. Metal acetylacetonate complexes are widely used as catalysts and reagents.

1.8.1 Copper (II) Acetylacetonate

Copper(II) acetylacetonate prepared by treating acetylacetonone with aqueous $\text{Cu}(\text{NH}_3)_4^{2+}$ and is available commercially, catalyst coupling and carbene transfer reactions. Quickly, easily and acetyl acetone in basic solution of aqueous copper (II) sulfate from the reaction can be isolated as a blue solid product can be prepared. Structural formula of copper acetylacetonate is given in Figure 1.7.

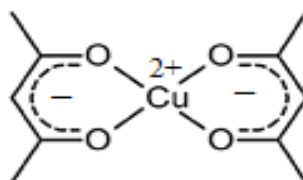


Figure 1.7 Copper (II) acetylacetonate

1.9 The Purpose of the Study

It has been well known that $\text{Cu}(\text{acac})_2$ was used itself as homogeneous catalyst. To carry out the reactions without using the solvents, in recent years, due to the Green Chemistry concept, it is common to use heterogeneous catalytic reactions instead of homogeneous ones. In the present work, Bentonite clay in the smectite group, which contains the main mineral of montmorillonite (:natural smectite, natural product) and Siral 80 (synthetic analogue of bentonite, silica-alumina), were used as supports for the active catalyst copper (II) acetylacetonate. The complex was

immobilized onto the surfaces of the clays after functionalisation with (3-aminopropyl)triethoxysilane (APTES). To assess the effectiveness of this procedure, the complex was also directly immobilized onto the unmodified clays. All the materials were characterized by X-Ray Fluorescence (XRF), Thermogravimetric Analyses (TGA/DTG), X-Ray Powder Diffraction (XRD), Scanning Electron Microscope (SEM), Atomic Absorption Spectroscopic (AAS), Specific Surface Area Determination (BET) and Fourier Transform Infrared (FTIR).

CHAPTER TWO

EXPERIMENTAL STUDIES

2.1 Materials, Reagents and Solvents

Bentonite was supplied from natural product, purchased from BENSAN A.Ş. (Enez/Edirne-Turkey), and Siral 80 was purchased from Sasol-Condea AG/Germany. The compound (3-aminopropyl)triethoxysilane (APTES) (09324), were purchased from Fluka, copper (II) acetylacetonate (02712), chloroform (02431) was from Merck and toluene (32249) were purchased from Riedel-de Haën.

2.2 Preparation of Clay Samples

The catalysts are prepared according to the literature procedure which is given shortly below (Pereira et al., 2007).

2.2.1 Functionalisation of the Clay with (3-aminopropyl)triethoxysilane

Prior to use, Bentonite/Siral 80 was heated in an oven at 120 °C for 1 h, in an oven. Afterwards clay (2.00 g) in dry toluene (100 cm³) and 1.18 cm³ of (3-aminopropyl) triethoxysilane (5.06 mmol) was refluxed for 24 h. The resulting material (Bentonite-APTES / Siral 80-APTES) was filtered by vacuum, refluxed with dry toluene (100 cm³) for 2 h, and then dried in an oven at 110 °C under vacuum for 3 h (Scheme 1a).

2.2.2 Anchoring of Copper (II) Acetylacetonate onto APTES Functionalized Clay

A solution of Cu(acac)₂ (0.0236 g, 90 µmol) in chloroform (50 cm³) was refluxed with APTES functionalized Bentonite/Siral 80 (0.60 g) for 24 h. The resulting solid was filtered by vacuum, refluxed with chloroform (50 cm³) for 2 h, recovered by vacuum filtration, and then dried in an oven at 110 °C for 3 h in an oven (Scheme

1b). These material will be referred to as Bentonite-APTES-Cu(acac)₂/ Siral 80-APTES-Cu(acac)₂.

2.2.3 Direct Anchoring of Copper (II) Acetylacetonate onto Clay

A solution of Cu(acac)₂ (0.0236 g, 90 μmol) in chloroform (50 cm³) was refluxed with Bentonite/Siral 80 (0.60 g) for 24 h. The resulting solid was filtered by vacuum, refluxed with chloroform (50 cm³) for 2 h, recovered by vacuum filtration, and then dried in an oven at 110 °C for 3 h in an oven (scheme 1.c) . These material will be labeled as Bentonite-Cu(acac)₂ / Siral 80-Cu(acac)₂ .

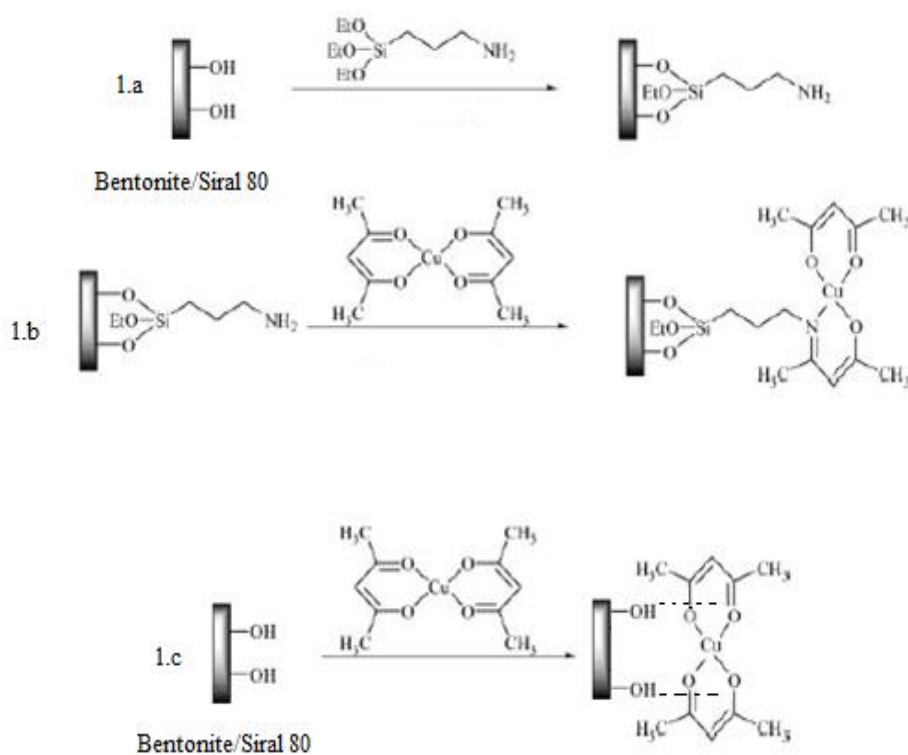


Figure 2.1 Bentonite / Siral 80 carriers with Cu(acac)₂ catalyst preparation

2.3. Characterization of the Samples

All of the materials were characterized by XRF, TGA/DTG, XRD, SEM, AAS, BET and FTIR.

2.3.1 X-Ray Fluorescence (XRF) Analysis

Chemical components of Bentonite and Siral 80 were measured on X-Ray Fluorescence (XRF) Spectra IQ2.

2.3.2 B.E.T Specific Surface Area Determination

Surface area is related to the adsorption capacity of an adsorbent. The multipoint BET surface area analysis of powder form of the samples was performed with Quantachrome Autosorb Automated Gas Sorption System. The analysis is carried out through an adsorption of N₂ gas. The specific surface areas of clays and modified clays were determined by using BET method after N₂ adsorption–desorption at 77 K with Sorptomatic 1990, Darmstadt Technical University, Germany. Before the adsorption experiments the samples were outgassed under vacuum for two hours at 130 °C.

2.3.3 Atomic Absorption Spectroscopic (AAS) Analysis

The bulk copper contents were determined by atomic absorption spectroscopy in a Perkin Elmer AAnalyst 700. Samples (20 mg) were previously dried at 100 °C, mixed with aqua regia (2 cm³) and HF (3 cm³) for 1 h at 120 °C, in a stainless-steel autoclave equipped with a polyethylene-covered beaker. After cooling to room temperature, the solution was mixed with boric acid (about 2 g) and finally adjusted to a known volume with deionised water.

2.3.4 X-Ray Powder Diffraction (XRD) Analysis

X-ray diffractograms (XRD) were obtained with oriented mounts, in a Phillips X'Pert Pro instrument using Cu K_{α} radiation and range for Bentonite $2\theta = 3-10^{\circ}$, range for Siral 80 $2\theta = 3-70^{\circ}$.

2.3.5 Thermogravimetric Analysis (TGA/DTG)

TGA/DTG was performed under nitrogen flow and atmosphere air from room temperature to 1000 °C at a rate of 10 °C/min with a Perkin Elmer Diamond TGA/DTG instrument. As a result of thermogravimetric analysis are included in the section.

2.3.6 Fourier Transform Infrared (FTIR) Analysis

Fourier transform infrared (FTIR) spectra (transmission) were measured on a Perkin-Elmer FTIR spectrophotometer Spectrum BX-II in the range 4000-400 cm^{-1} at a resolution of 4 cm^{-1} and 24 scan. The spectra of the solids were obtained in KBr pellets (Fluka, spectroscopic grade), with 4% dilution.

2.3.7 Scanning Electron Microscope (SEM) Analysis

The structure and agglomeration of Bentonite before and after the modification were investigated by scanning electron microscopy (SEM) using a JEOL JSM-6060 microscope with gold coating at an acceleration voltage of 20 kV.

CHAPTER THREE

RESULTS

3.1 Results

The complex, $\text{Cu}(\text{acac})_2$ was immobilized onto the surface of amine-functionalized clay, Bentonite and Siral 80, by a two-step procedure involving:

- (a) functionalisation of the parent clays with (3-aminopropyl)triethoxysilane, resulting in clays surface with free amine groups;
- (b) anchoring of copper (II) acetylacetonate by reaction between the free amine clay groups and the carbonyl groups of the acetylacetonate ligand.

To assess the effectiveness of this method, $\text{Cu}(\text{acac})_2$ was also directly immobilized onto the unmodified clays.

3.1.1 X-Ray Fluorescence (XRF) Results

Chemical composition analysis of Bentonite and Siral 80 were given in Table 3.1 and Table 3.2, as a result of XRF Analysis, respectively.

Table 3.1 Chemical components of Bentonite

Component	SiO ₂	Al ₂ O ₃	Fe ₂ O ₃	TiO ₂	CaO	MgO	Na ₂ O	K ₂ O ₃	*LOI
(%) Weight	45.42	12.01	3.61	0.44	7.24	3.65	1.41	1.64	24.58

* Loss of Ignition

Table 3.2 Chemical components of Siral 80

Component	SiO ₂	Al ₂ O ₃	Fe ₂ O ₃	TiO ₂	CaO	MgO	Na ₂ O	K ₂ O ₃	*LOI
(%) Weight	60.23	16.70	0.02	0.02	0.01	0.22	2.09	0.01	20.67

* Loss of Ignition

The samples were composed of basically silica and alumina. Bentonite can be evaluated as iron rich Bentonite.

3.1.2 Cu (II) the Determination with Atomic Absorption Spectroscopy (AAS)

Results

Theoretical copper content of copper (II) acetylacetonate was calculated as follows:

$$\text{Copper content of copper (II) acetylacetonate for 0.0236 g} = \frac{(\text{used copper (II) acetylacetonate}) \times (\text{M.W. of copper})}{(\text{M.W. of copper (II) acetylacetonate})}$$

$$\text{Copper content of copper (II) acetylacetonate for 0.0236 g.} = \frac{(0.0236) \times (63.546)}{(261.77)}$$

Copper content of copper (II) acetylacetonate for 0.0236 g = 5.72×10^{-3} g.

$$\text{Copper content for 1 g.} = \frac{(1 \text{ g.}) \times (\text{copper content of copper (II) acetylacetonate})}{(\text{Weight of catalyst sample})}$$

$$\text{Copper content for 1 g.} = \frac{(1 \text{ g.}) \times (5.72 \times 10^{-3} \text{ g.})}{(0.623 \text{ g.})}$$

Copper content for 1 g. = 9.18×10^{-3} g. = 9180 $\mu\text{g/g}$

$$\text{Copper content for 1g. of catalyst samples} = \frac{(\text{copper ppm concentration in AAS}) \times (\text{a known volume with deionised water}) \times (1 \text{ g.})}{(\text{Amount of used catalyst samples})}$$

Table 3.3 Copper concentrations of catalyst samples in AAS Analysis

Sample	Copper Concentration (ppm)
Bentonit-Cu(acac) ₂	2.51
Bentonit-APTES-Cu(acac) ₂	1.82
Siral 80-Cu(acac) ₂	2.42
Siral 80-APTES-Cu(acac) ₂	0.76

- Theoretical copper content of copper acetylacetonate: $9180 \mu\text{g/g}$
- Amount of Cu(II) in Bentonite-Cu(acac)₂ catalyst: $6275 \mu\text{g/g}$
- Amount of Cu(II) in Bentonite-APTES-Cu(acac)₂ catalyst: $4550 \mu\text{g/g}$
- Amount of Cu(II) Siral 80-Cu(acac)₂ catalyst: $6050 \mu\text{g/g}$
- Amount of Cu(II) Siral 80-APTES-Cu(acac) catalyst: $1900 \mu\text{g/g}$

As can be seen from Table 3.3, the amounts of copper in Bentonite-Cu(acac)₂ and Siral 80-Cu(acac)₂ catalysts were higher than the other samples due to the fact that the direct immobilization of Cu(acac)₂ via –OH functional groups of Bentonite and Siral 80. On the other hand, in the case of Bentonite-APTES-Cu(acac)₂ and Siral 80-APTES-Cu(acac)₂ samples, the amounts of copper is less than the other catalysts. This may be the bounding of Cu(acac)₂ complex over only NH₂ group of APTES.

3.1.3 B.E.T. Analyses Results

BET specific surface areas values of the samples were given in Table 3.4 after N₂ adsorption-desorption at 77K. These measurements were done in TU-Darmstadt/Germany.

Table 3.4 B.E.T. Analyses of Catalysts

Samples	A _{BET} (m ² /g)
Bentonite	65
Bentonite-Cu(acac) ₂	48
Bentonite-APTES-Cu(acac) ₂	38
Siral 80	238
Siral 80-APTES-Cu(acac) ₂	77
Siral 80-Cu(acac) ₂	55

3.1.4 Fourier Transform Infrared (FTIR) Spectra Results

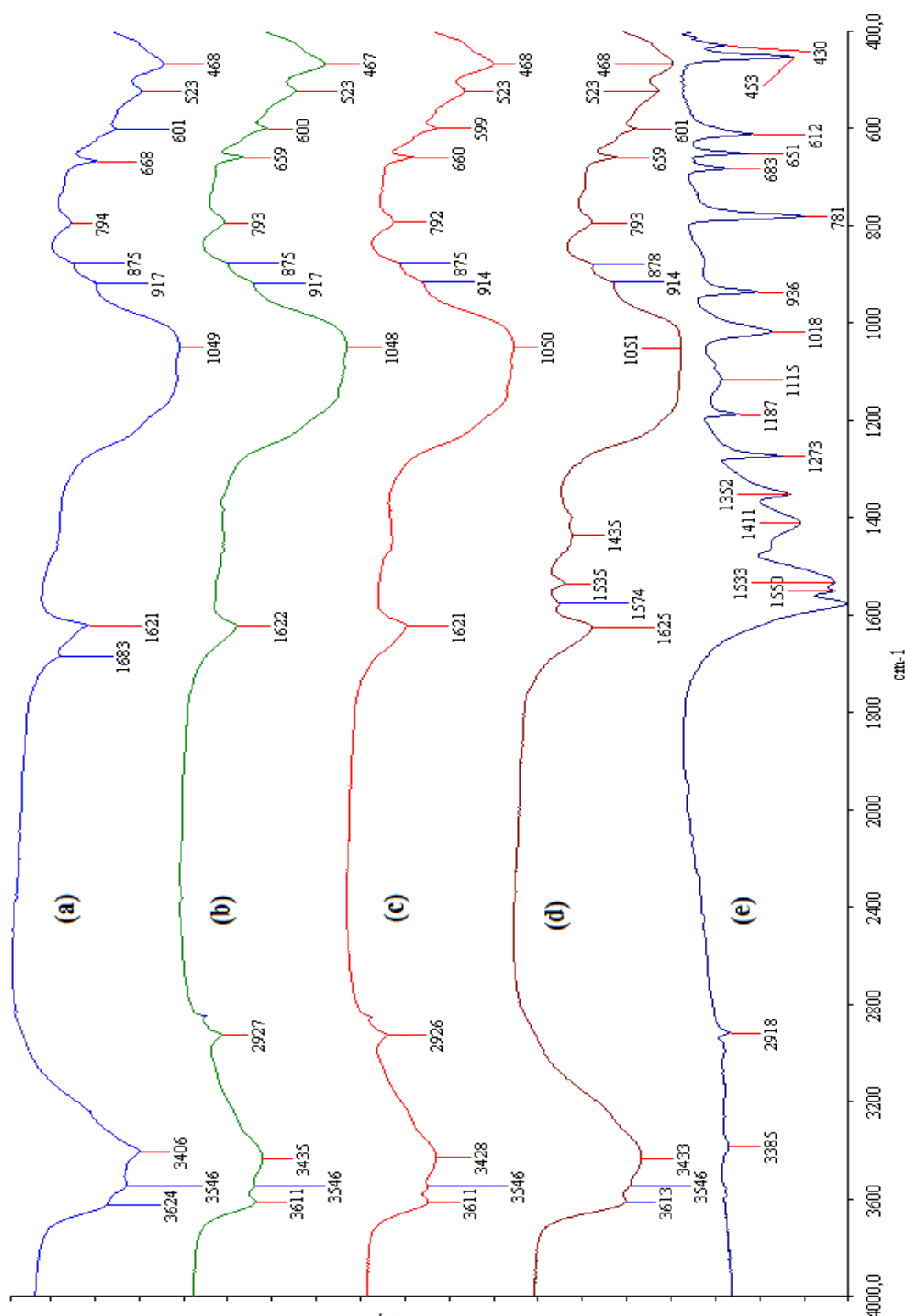


Figure 3.1 The FTIR spectra of (a) Bentonite, (b) Bentonite-APTES, (c) Bentonite-APTES-Cu(acac)₂, (d) Bentonite-Cu(acac)₂, (e) Cu(acac)₂ were performed in the range of 4000–400 cm⁻¹.

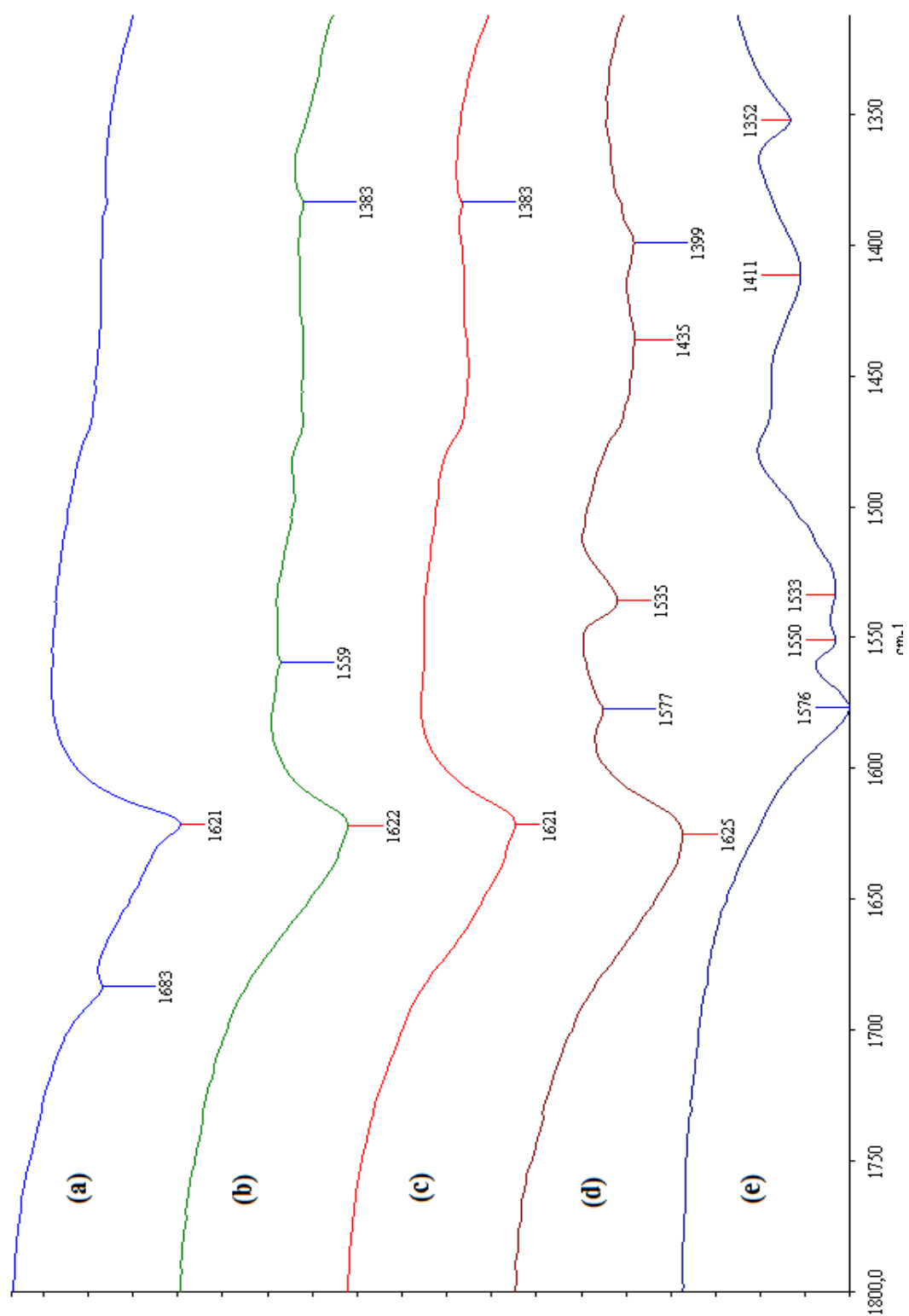


Figure 3.2 The FTIR spectra of (a) Bentonite (b) Bentonite-APTES (c) Bentonite-APTES- $\text{Cu}(\text{acac})_2$ (d) Bentonite- $\text{Cu}(\text{acac})_2$ (e) $\text{Cu}(\text{acac})_2$ were performed in the range of 1800–1300 cm^{-1}

The FTIR spectra of the Bentonite based materials, presented in Figure 3.7 show in the range 3546–3406 cm^{-1} two components associated with -OH stretching vibrations for Bentonite from Montmorillonite (physisorbed water) (Caglar et al., 2005), it shows a peak at approximately 3624 cm^{-1} corresponding to -Al-Mg-OH stretching vibration (Caglar et al., 2005). The band at around 1621 cm^{-1} also corresponds to the -OH deformation of water to observe natural Bentonite (Tabak et al., 2007). The band at 1049 cm^{-1} is attributed to -Si-O stretching (in-plane) vibration for layered silicates. IR peaks at 917 and 878 cm^{-1} are attributed to Al-Al-OH and Al-Mg-OH bending vibration deformation bands respectively (Araujo et al., 2004). In the IR studies of Bentonite, the Si-O stretching vibrations were observed at 794 cm^{-1} and 668 cm^{-1} showing the presence of Silica and Quartz (Pereira et al., 2008, Katsioti et al., 2008). The bands at 523 and 468 cm^{-1} are due to Si-O-Al (octahedral) and Si-O-Si bending vibrations respectively, for each sample (Tabak et al., 2007).

After APTES grafting onto Bentonite several changes can be observed in all the spectra frequency range. The bands at 3406 cm^{-1} corresponding to -OH stretching vibrations for Bentonite, there was an overall intensity decrease of the broad band, due to a decrease in the interlayer water content, as a consequence of the grafting reaction of APTES onto the M-OH clay surface groups. The new band was detected at 3435 cm^{-1} in Bentonite-APTES. In the ranges 2927 cm^{-1} , there was a new band associated with the -CH₂ stretching vibrations from grafted APTES (Caglar et al., 2005). The band due to -NH₂ stretching could not be observed, as it was masked by the broad OH stretching band. This band observed at 1559 cm^{-1} (Alemdar et al., 2000). C-N ring stretching (skeletal) vibrations in the Bentonite-APTES was observed at 1383 cm^{-1} which result from silan but this band was not observed in the natural Bentonite (Tabak et al., 2007). The Si-O stretching vibrations were observed at 668 cm^{-1} and new bands are detected at 659 cm^{-1} , the Si-O was changed -Si-CH₂-R.

The FTIR spectra of copper acetylacetonate anchored onto Bentonite-APTES showed a similar band pattern and were presented in Figure 3.2. The band for -CH₂

stretching vibrations from APTES at about 2926 cm^{-1} still appeared in Bentonite-APTES-Cu(acac)₂ at unaltered frequencies compared to their parent materials (Pereira, 2008). In the range of aliphatic C–H stretching vibrations ($2900\text{--}2700\text{ cm}^{-1}$) no significant changes were observed, even though Cu complex vibrations were expected to occur at the same frequencies in Bentonite-APTES-Cu(acac)₂. The band for aliphatic C=C- stretching vibrations from Cu(acac)₂ at $1500\text{--}1600\text{ cm}^{-1}$ appeared. The band assigned to –NH₂ bending vibration (1558 cm^{-1} in Bentonite-APTES) decreased in intensity and new band was detected at 1435 cm^{-1} in Bentonite-APTES-Cu(acac)₂. C-N bending vibration was detected at 1383 cm^{-1} . It was noticeable in the spectra was an increase in the intensities and broadness of the bands. In this context, the new bands/shoulders may be attributed to the anchored complex and assigned to stretching vibrations associated with the new C=N bond formed by Schiff condensation reaction between the amine groups of the grafted APTES onto Bentonite the C=O group from the coordinated acetylacetonate ligand (Pereira et al., 2007). On the other hand, interaction of APTES functionalised clay with Cu(acac)₂ may be explained as the formation of NH bond in intermediate step by the opening of (acac) ring. After that formation of C=N bond by the elimination of H₂O and closing the ring. In fact, a Mg-phyllsilicate sequentially functionalised with APTES and acac ligand showed a band at 1608 cm^{-1} which was assigned to $\nu(\text{C}=\text{N})$, that after copper complexation showed a shift to approximately 1633 cm^{-1} (Lagadic, 2006).

The expected increase in band broadness in the region of $3400\text{--}3700\text{ cm}^{-1}$ due to the hydroxyl groups being in hydrogen bond interaction (Pereira et al., 2008) was not detected for Bentonite-Cu(acac)₂, and a possible explanation for this was that some of the complexes might have also related with –OH groups via the ligand-exchange mechanism with the formation of a Cu–O–Clay bond (tetrahedral species) or/and by axial coordination of the metal centre to the hydroxyl surface groups. As well as specific Cu(acac)₂ bands were observed at 1574 cm^{-1} for –C–C–, 1535 cm^{-1} for –C–O–, and 1399 cm^{-1} for –CH₃, respectively.

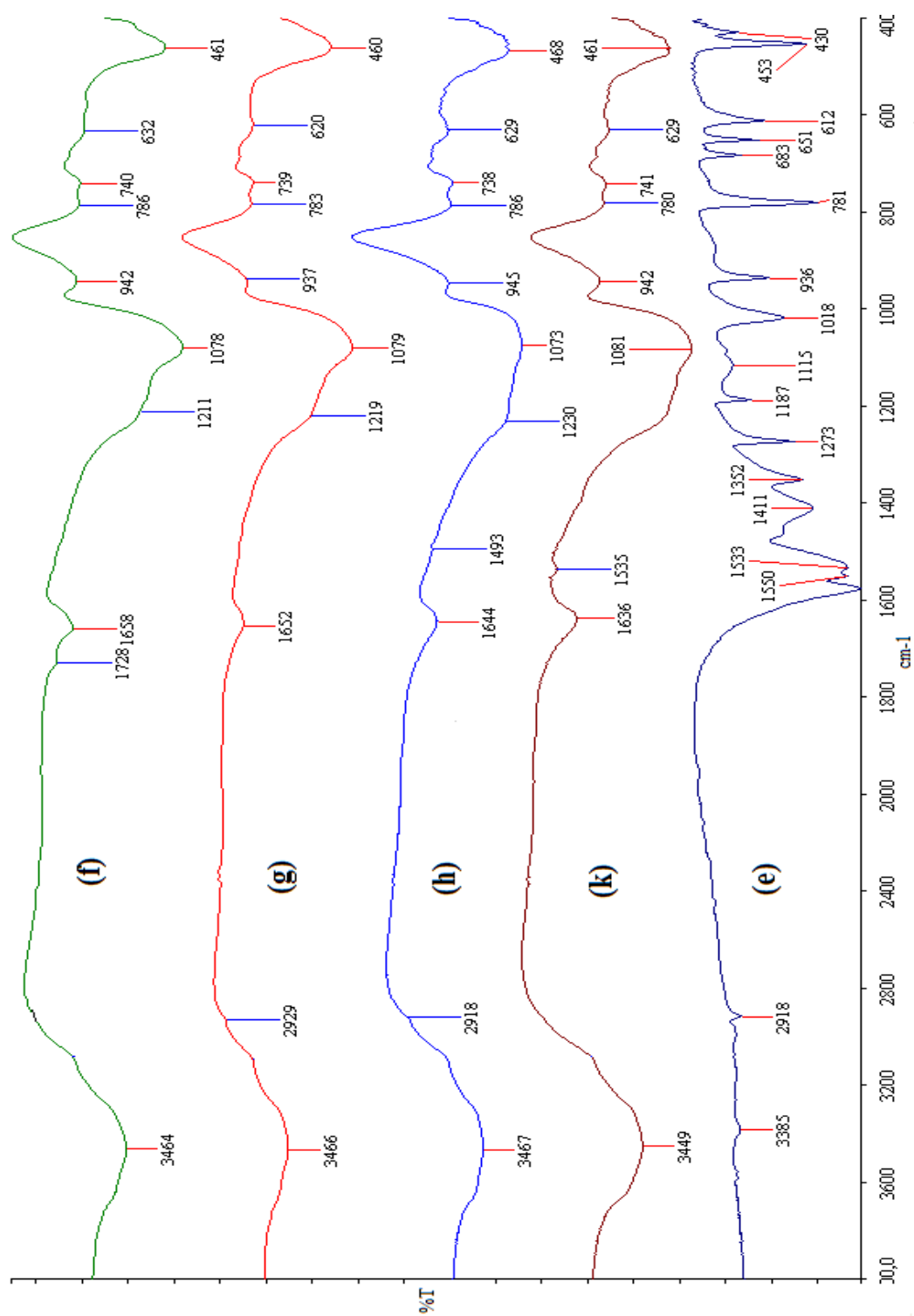


Figure 3.3 The FTIR spectra of (f) Siral 80, (g) Siral 80-APTES (h) Siral 80-APTES-Cu(acac)₂ (k) Siral 80-Cu(acac)₂ (e) Cu(acac)₂ were performed in the range of 4000–400 cm^{-1}

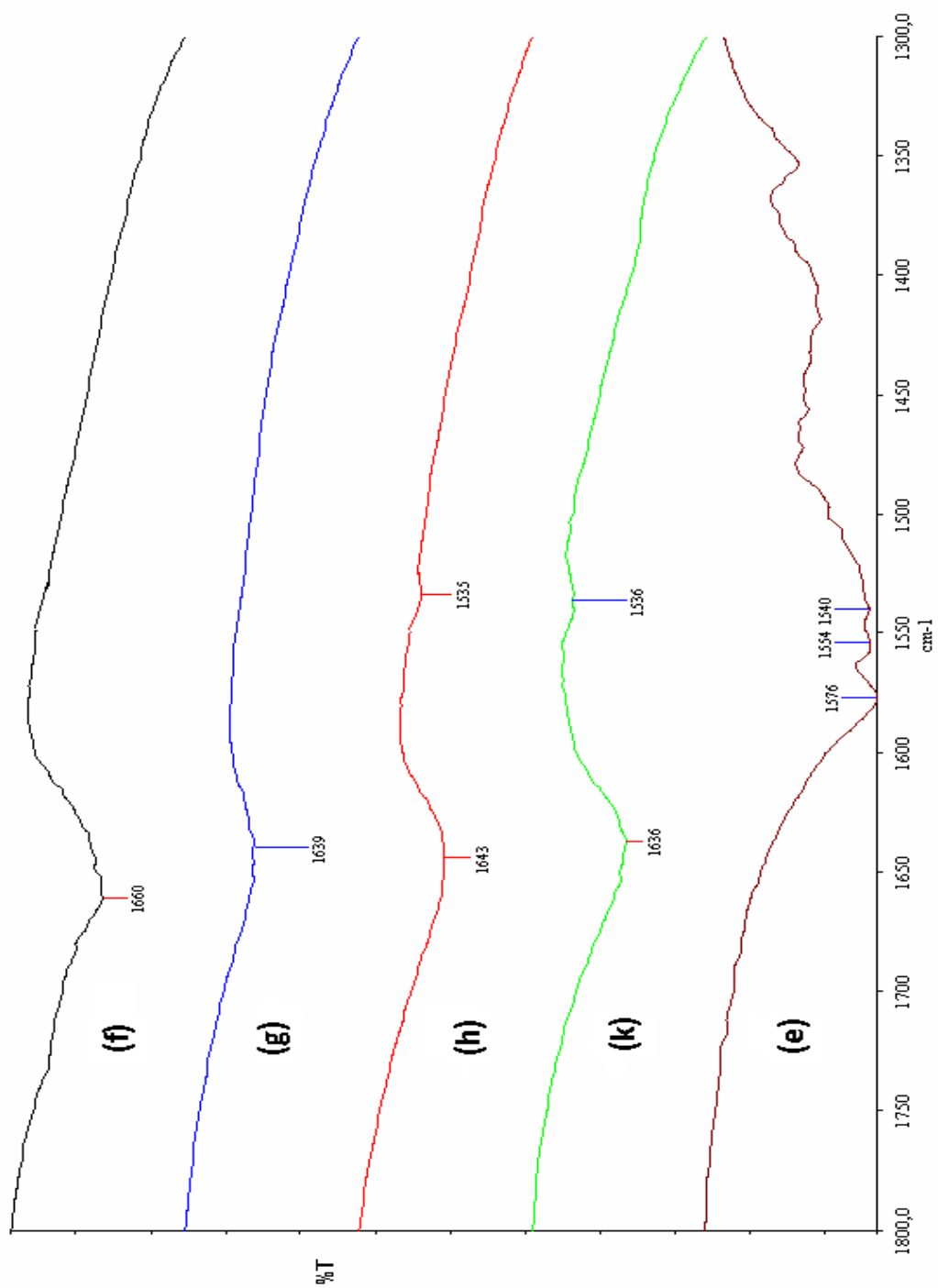


Figure 3.3 The FTIR spectra of (f) Siral 80, (g) Siral 80-APTES (h) Siral 80-APTES- $\text{Cu}(\text{acac})_2$ (k) Siral 80- $\text{Cu}(\text{acac})_2$ (e) $\text{Cu}(\text{acac})_2$ were performed in the range of $1800\text{--}1300\text{ cm}^{-1}$

Figure 3.8 showed FTIR spectra of Siral 80 and immobilized onto the unmodified and the modified clays. As can be seen, the spectra of Siral 80 contained the bands corresponding to stretching of -OH at 3464 cm^{-1} . The band at around 1660 cm^{-1} also corresponded to the -OH deformation(:bending) of water observed for Siral 80. The band at 1049 cm^{-1} was attributed to -Si-O stretching (in-plane) vibration for layered silicates. The bands at around 942 cm^{-1} were attributed to M-OH bending vibration deformation bands respectively. The Si-O stretching vibrations were observed at 786 cm^{-1} , 740 cm^{-1} and 632 cm^{-1} . These were reflected the presence of Silica and Quartz. The bands at 461 cm^{-1} was corresponded to Si-O-Si bending vibrations (Yurdakoç et al., 2005).

After APTES grafting onto Siral 80, there was no changes in bands for -OH stretching vibrations. The bands at 3466 cm^{-1} for Siral 80-APTES. In the ranges 2929 cm^{-1} , there is new band associated with the -CH_2 stretching vibrations from grafted APTES. The band due to -NH_2 stretching could not be observed, as it was masked by the broad -OH bending band. The band at 1539 cm^{-1} was observed. In the case of Copper acetylacetonate anchored onto Siral 80-APTES, -CH_2 stretching vibrations band from APTES at 2918 cm^{-1} still appeared. The band for aliphatic C=C- stretching vibrations from $\text{Cu}(\text{acac})_2$ at $1500\text{-}1600\text{ cm}^{-1}$ also observed. The band due to -NH_2 was not detected. C-N bending vibration was seen at 1220 cm^{-1} . The band at around 1536 cm^{-1} for -C-O- in Siral 80- $\text{Cu}(\text{acac})_2$ catalyst sample was also observed (Daniell et al., 2000).

3.1.5 X-ray Diffractograms (XRD) Results

XRD diffraction patterns of the samples were given in Figure 3.5 and Figure 3.6. XRD Data were also presented in Table 3.5 and 3.6.

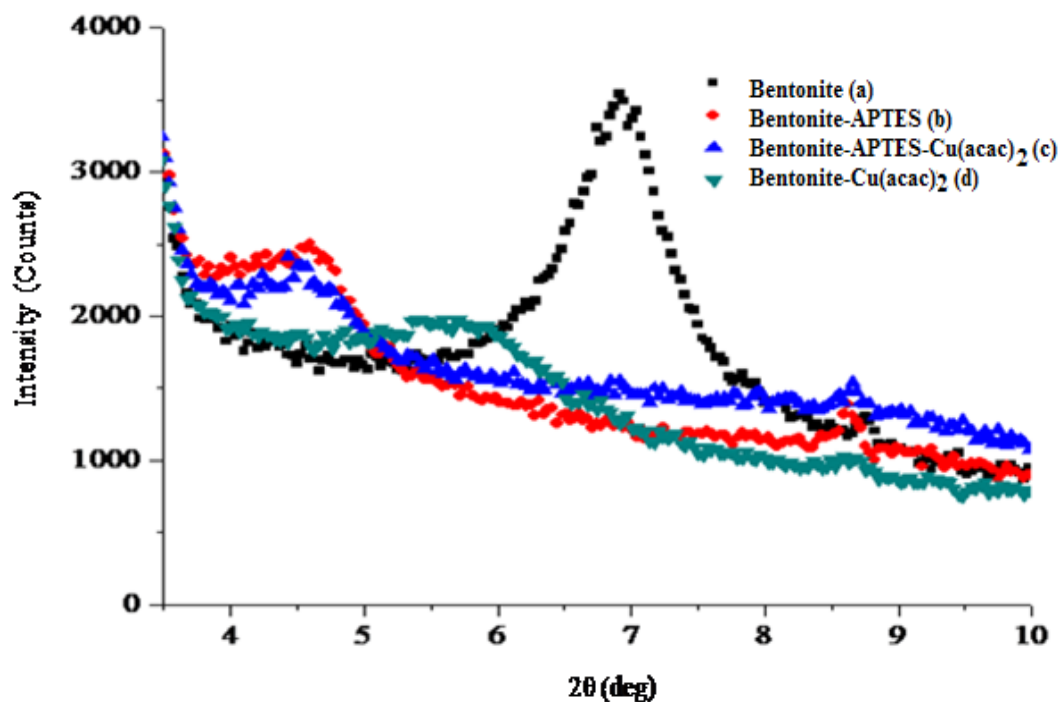


Figure 3.5 XRD Results a) Bentonite b) Bentonite-APTES c) Bentonite-APTES-Cu(acac)₂ d) Bentonite-Cu(acac)₂

Table 3.5 XRD of Bentonite Supported Catalysts

	[°2θ]	Height [cts]	FWHM [°2θ]	d-spacing [Å]
Bentonite	6.97	1949.12	0.58	12.67
Bentonite-APTES	4.67	990.18	0.39	18.92
Bentonite-APTES-Cu(acac)₂	4.59	726.42	0.52	19.28
Bentonite-Cu(acac)₂	5.80	417.30	0.91	15.23

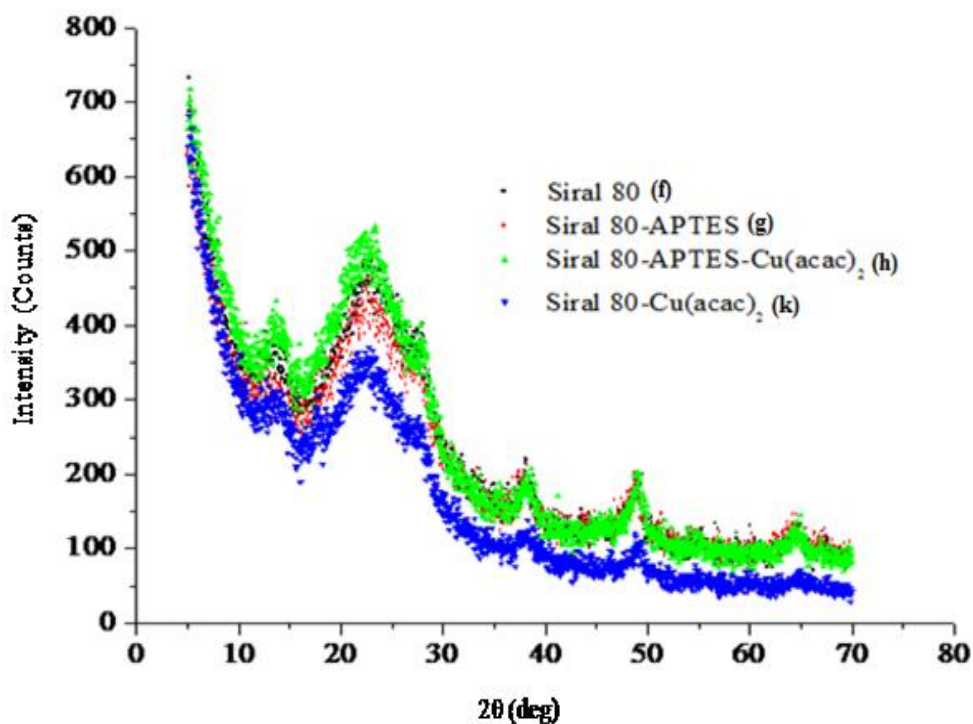


Figure 3.6 XRD Results f) Siral 80 g) Siral 80-APTES h) Siral 80-APTES-Cu(acac)₂
k) Siral 80-Cu(acac)₂

Table 3.6 XRD of Siral 80 Supported Catalysts

	[°2θ]	Height [cts]	FWHM [°2θ]	d-spacing [Å]
Siral 80	14.08	410.02	0.56	6.29
Siral 80-APTES	12.87	103.82	0.34	6.88
Siral 80-APTES- Cu(acac)₂	13.46	127.52	0.03	6.58
Siral 80-Cu(acac)₂	13.60	90.50	0.15	6.51

According to the results, the main structures of Bentonite and Siral 80 were conserved.

3.1.6 Thermogravimetric Analyses (TGA/DTG) Results

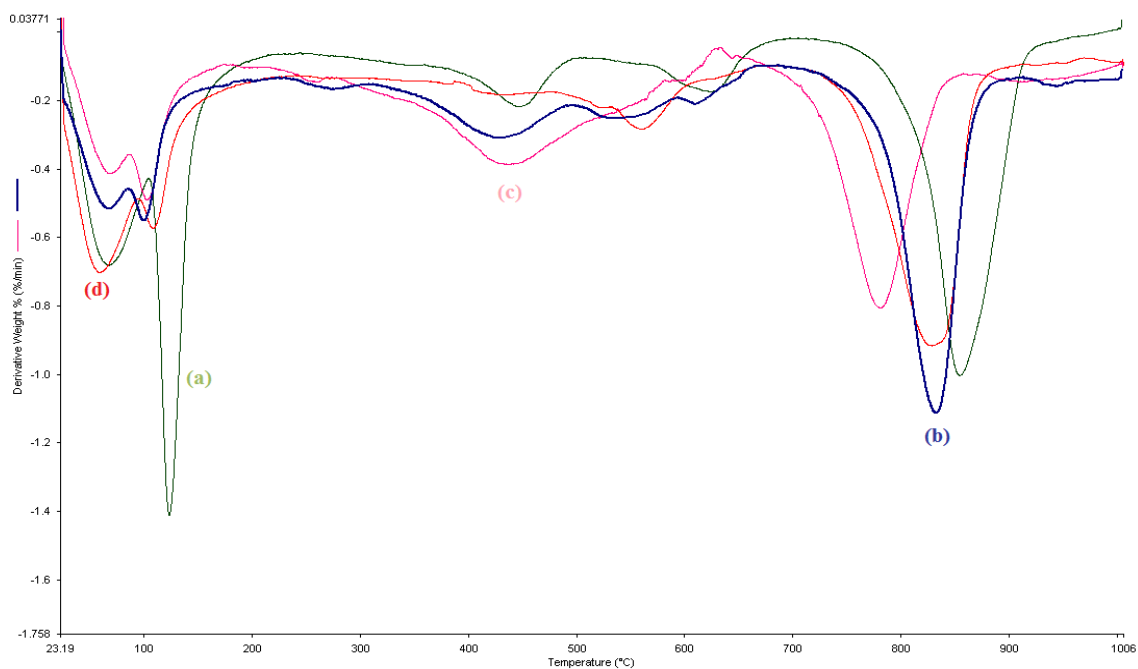
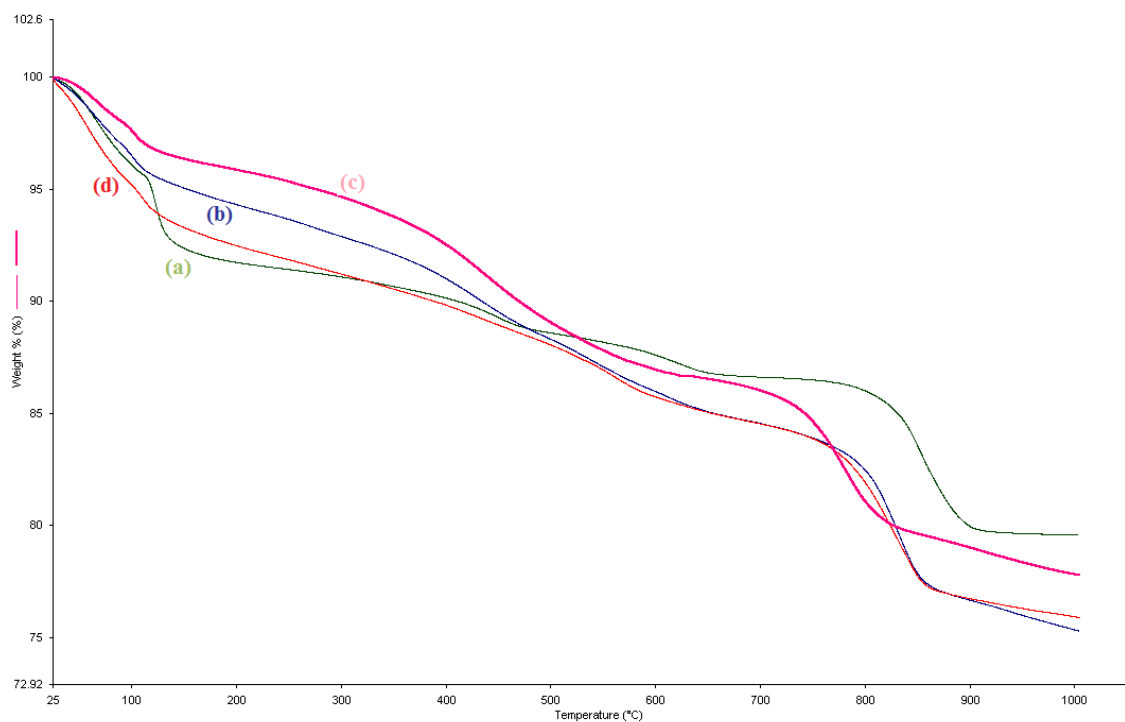


Figure 3.7 TGA/DTG profiles of a) Bentonite b) Bentonite-APTES c) Bentonite-APTES-Cu(acac)₂ d) Bentonite-Cu(acac)₂

TGA/DTG thermograms (curve or profile) of Bentonite samples were shown in Figure 3.7. TGA/DTG profile of the original sample (Bentonite) showed three main steps of mass losses. In the first step, two dehydration stages with a total mass loss of 8.52% over the temperature range of 25–250 °C are noticeable on the TGA/DTG curve of Bentonite (Fig 3.7 and Table 3.6). The removal of adsorbed water with a mass loss of 4.05 % in the first stage 25–105 °C and second step in the range of 105–250 °C which is accompanied by a mass loss of 4.47% corresponded to the elimination of the water species coordinated to the interlayer metal cations such as Na⁺ and Ca²⁺ on exchangeable sites in Bentonite. (Pereira et al., 2007, Caglar et al., 2008) The noticeable differences between the mass losses of untreated Bentonite in the temperature interval 250–710 °C were ascribed to the existence of external clay components such as Dolomite, α -Cristobalite, Quartz, Calcite, and Illite of Enez/Edirne Bentonite (Katsioti et al., 2008). Finally, a third main loss occurred at temperatures in the range 710–1000 °C, where the TGA/DTG curve displays a step mass loss (about 6.99%) related to the release of structural OH of natural Bentonite. The dehydroxylation temperature of about 854 °C was in agreement with the classical range of dehydroxylation temperature (700–900 °C) observed for Montmorillonites by Pereira et al., 2007.

In the curves for Bentonite-APTES (Fig. 3.7.b), the initial mass losses (about 7.22%) corresponded to adsorbed and interlayer water loss takes place. The TGA/DTG curve showed a slight gradual decrease in the range 25–310 °C, which was attributed to the water loss of Bentonite (Pereira et al., 2007). From the thermogravimetric curves for Bentonite-APTES, an estimation of the amount of grafted APTES could be made; in addition to, this estimation implied also some approximations, as previously discussed in the literature, namely that the APTES species decomposes as SiO₂, NH₃ and C₃H₆. In this context, and from the mass losses between 310 and 680 °C (Caglar et al., 2008), the mass losses in this temperature is about 7.99%. At the last part, the mass losses between clay layers adsorbed water was at the temperature range between 680–1000 °C and about 9.40%. The classical phase transition peak of Bentonite at 930 °C represented the decomposition of Dolomite impurity (Eren et al., 2008).

Immobilization of the $\text{Cu}(\text{acac})_2$ complexes onto the APTES modified clay showed three main step of mass losses. For all the sorbents, the mass loss at a temperature of less than 180 °C corresponds to loss of physisorbed and interlamellar water. This dehydration process is one of the characteristics of clay minerals. The mass losses of modified sorbents in this temperature range were less than that of Bentonite (3.93%) (Eren&Afsin, 2008). The specific group of silane had also mass losses and eliminated one part functional groups of $\text{Cu}(\text{acac})_2$ at the temperature range of 300-630 °C. At the last part, irreversible dehydroxylation of Bentonite occurred at 630-1000 °C, where mass loss was 8.84% .

In the case of Bentonit- $\text{Cu}(\text{acac})_2$, the removal of adsorbed water with a mass loss was about 8.67% in the first stage 25–300 °C which was accompanied by a mass loss of 4.3% corresponds to the elimination of the water species coordinated to the interlayer cations. The mass loss by 6.48% in the range of 300-680 °C originated from the dehydroxylation of amorphous smectites and eliminates functional groups of $\text{Cu}(\text{acac})_2$ (Araujo et al., 2004). The dehydroxylation of the compound seemed to take place after 700 °C. Total mass losses was 23.95%.

Table 3.7 TGA/DTG data of Bentonite Supported Catalysts

	1. Step	2. Step	3. Step	4. Step
	T.R (°C) / Mass	T.R (°C) / Mass	T.R (°C) / Mass	T.R (°C) / Mass
	Loss(%)	Loss(%)	Loss(%)	Loss(%)
Bentonite	25-250 / 8.52	250-520 / 2.98	520-710 / 1.83	710-1000 / 6.99
Bentonite-APTES	25-310 / 7.22	310-500 / 4.44	500-680 / 3.55	800-1000 / 9.40
Bentonite-APTES- Cu(acac)₂	25-180 / 3.93	300-630 / 9.38	630-1000 / 8.84	-
Bentonite-Cu(acac)₂	25-300 / 8.67	300-680 / 6.48	680-1000 / 8.80	-

T.R: Temperature Range

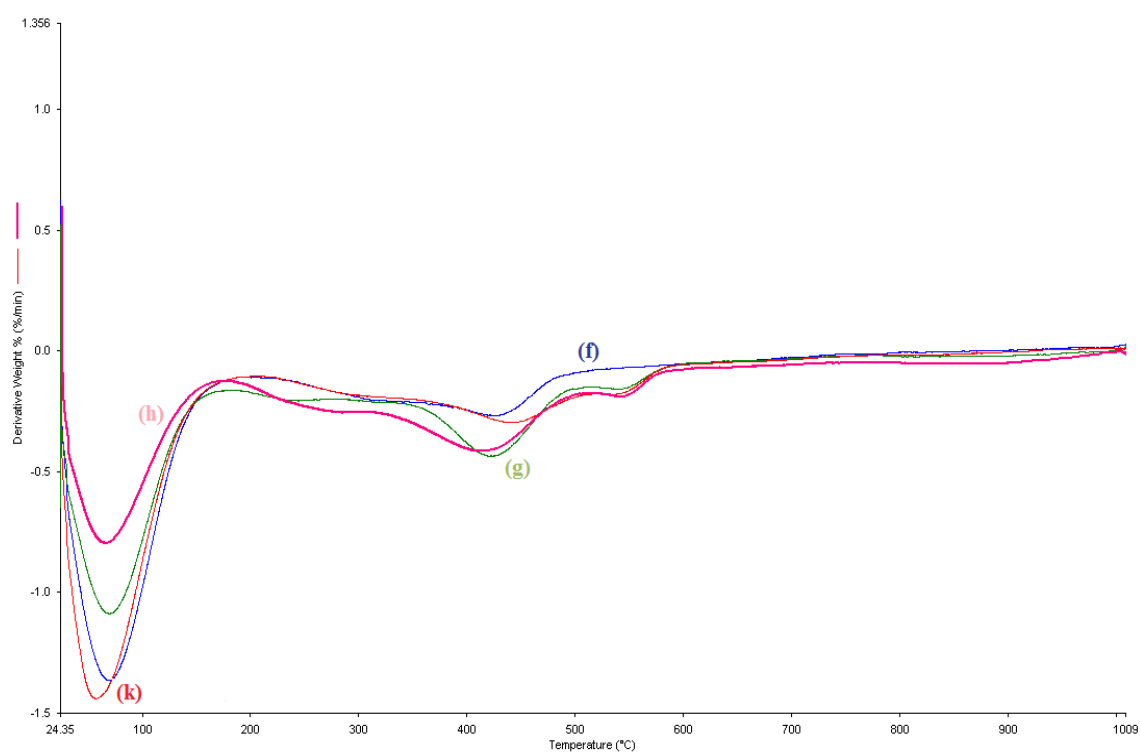
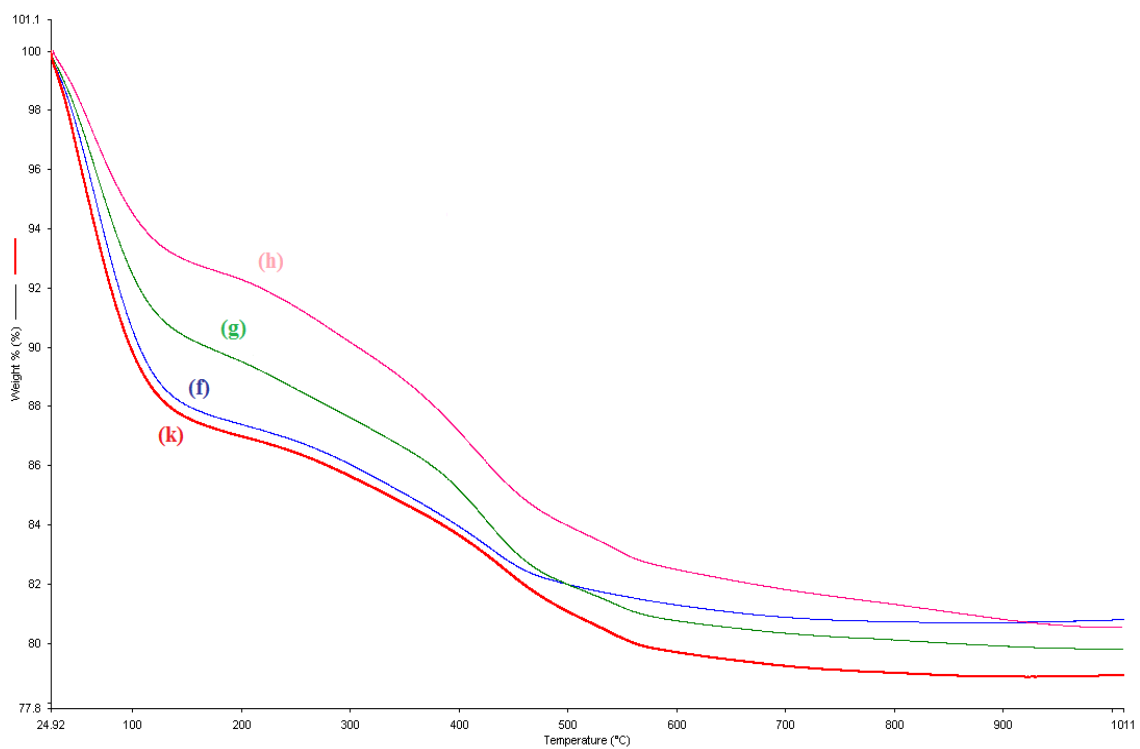


Figure 3.8 TGA/DTG profiles of f) Siral 80 g) Siral 80-APTES h) Siral 80-APTES-Cu(acac)₂ k) Siral 80-Cu(acac)₂

Siral 80 is a synthetic silica-alumina compound. The dehydration of Siral 80 occurred with a mass loss of 12.70% in the temperature range of 25–230 °C as a single-step process which gave rise to an endothermic maximum at 85 °C (Fig. 3.8) whereas this same process happened in two stages for raw Bentonite. A second main loss occurred at temperatures in the range 230–1000 °C, where the TGA/DTG curve displayed a step mass loss (about 6.28%) related to the release of structural OH of synthetic Siral 80.

In the curve of Siral 80-APTES (Fig. 3.8.g), the removal of adsorbed water with a mass loss was 10.37 % in the first stage 25–200 °C. In the TGA/DTG profiles of the other catalysts, thermogravimetric curves for second and third stage showed same decay, namely that the decomposition of APTES species as SiO₂, NH₃ and C₃H₆. However, the mass loss in the range of 200-500 °C originated from the dehydroxylation of amorphous smectites and eliminates functional groups of Cu(acac)₂.

Finally, the last main loss occurred in the temperature range of 500–1000 °C, this mass loss was attributed to evolution of the adsorbed water between the layers of catalysts.

Table 3.8 TGA/DTG data of Siral 80 Supported Catalysts

	1.Step	2. Step	3. Step	4. Step
	T.R (°C) / Mass Loss(%)	T.R (°C) / Mass Loss(%)	T.R (°C) / Mass Loss(%)	T.R (°C) / Mass Loss(%)
Siral 80	25-230 / 12.70	230-1000 / 6.28	-	-
Siral 80-APTES	25-200 / 10.37	200-300 / 1.89	300-510 / 5.78	500-1000 / 2.03
Siral 80-APTES- Cu(acac)₂	25-175 / 7.31	195-320 / 2.92	320-510 / 5.88	510-1000 / 3.26
Siral 80-Cu(acac)₂	25-200 / 12.94	200-360 / 2.47	380-510 / 3.63	500-1000 / 1.97

T.R: Temperature Range

3.1.7 Scanning Electron Microscope (SEM) Results

The SEM images of the samples were given below as in Figures 3.9-3.16.

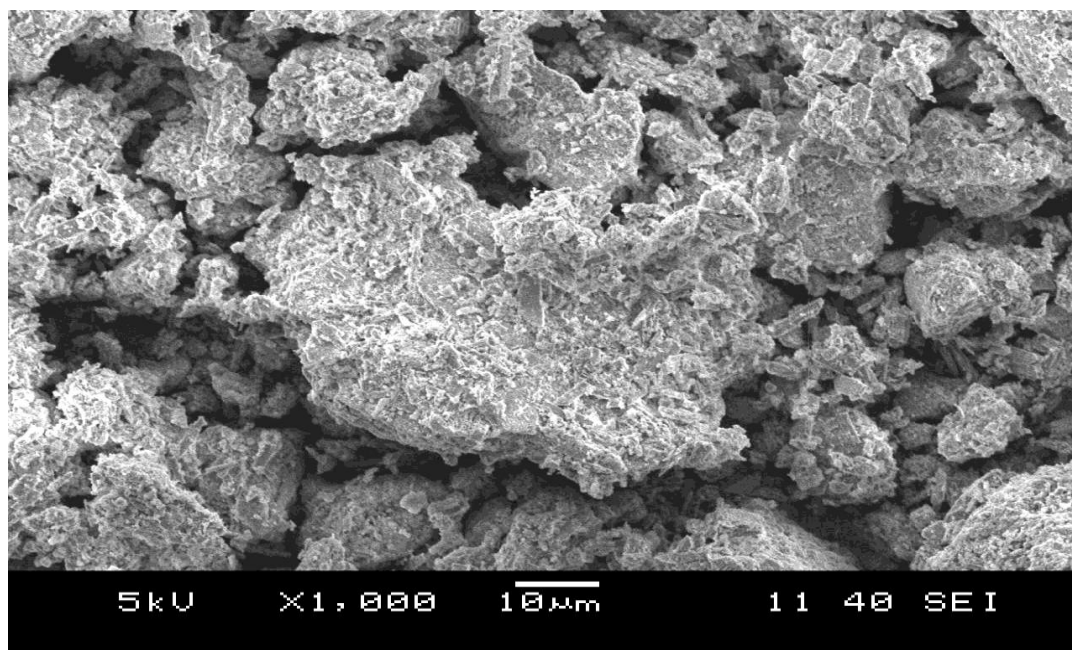


Figure 3.9. SEM Image of Bentonite

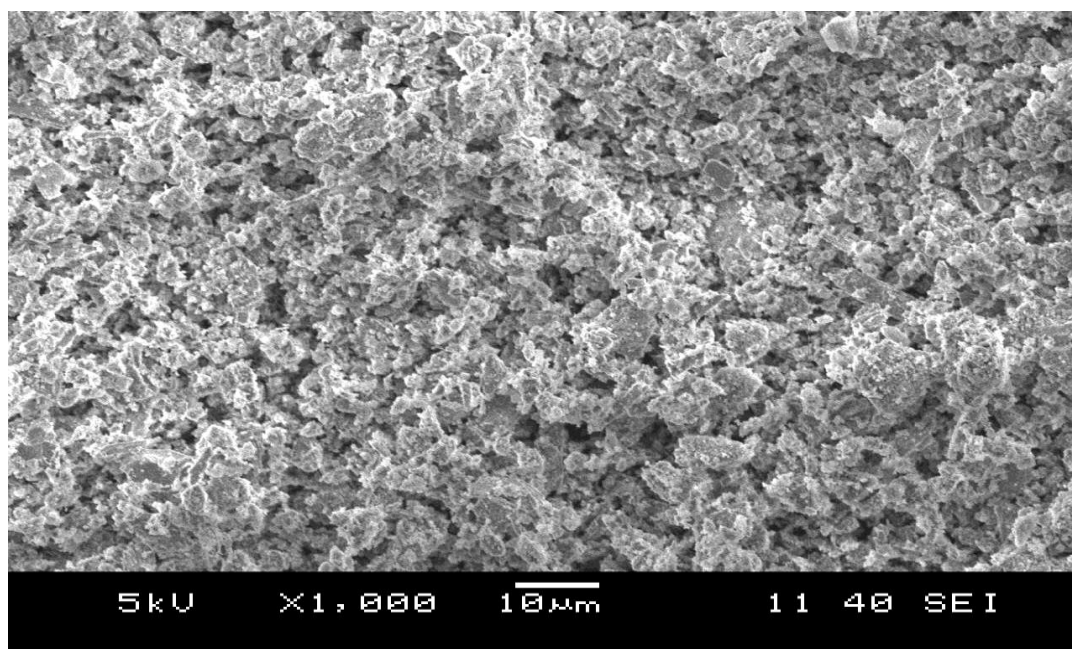


Figure 3.10. SEM Image of Bentonite-APTES

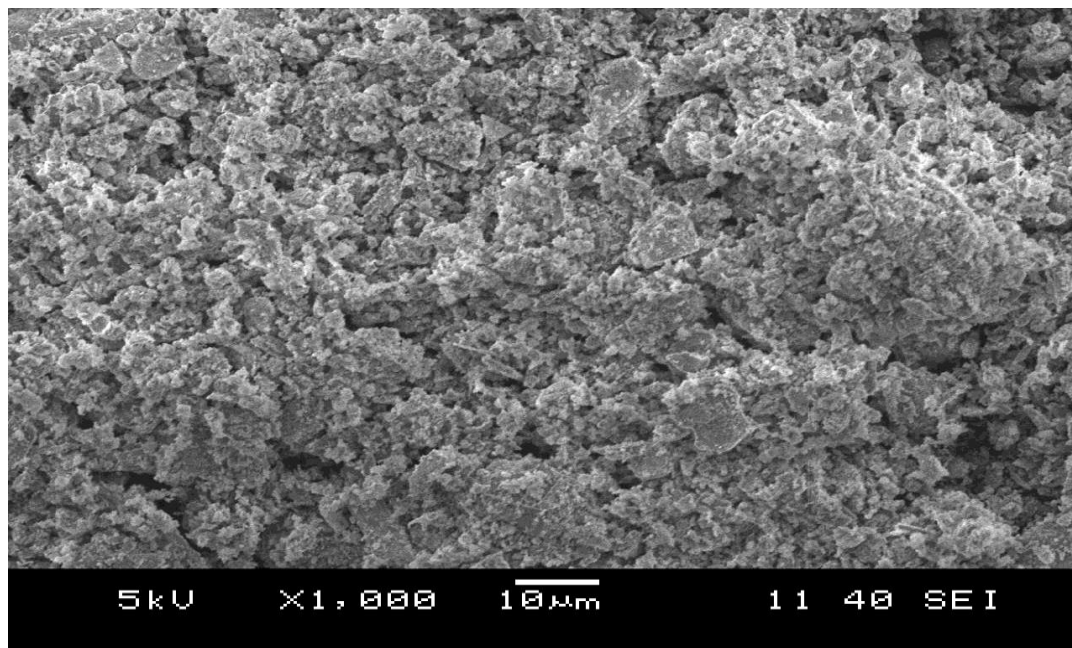


Figure 3.11. SEM Image of Bentonite-APTES-Cu(acac)₂

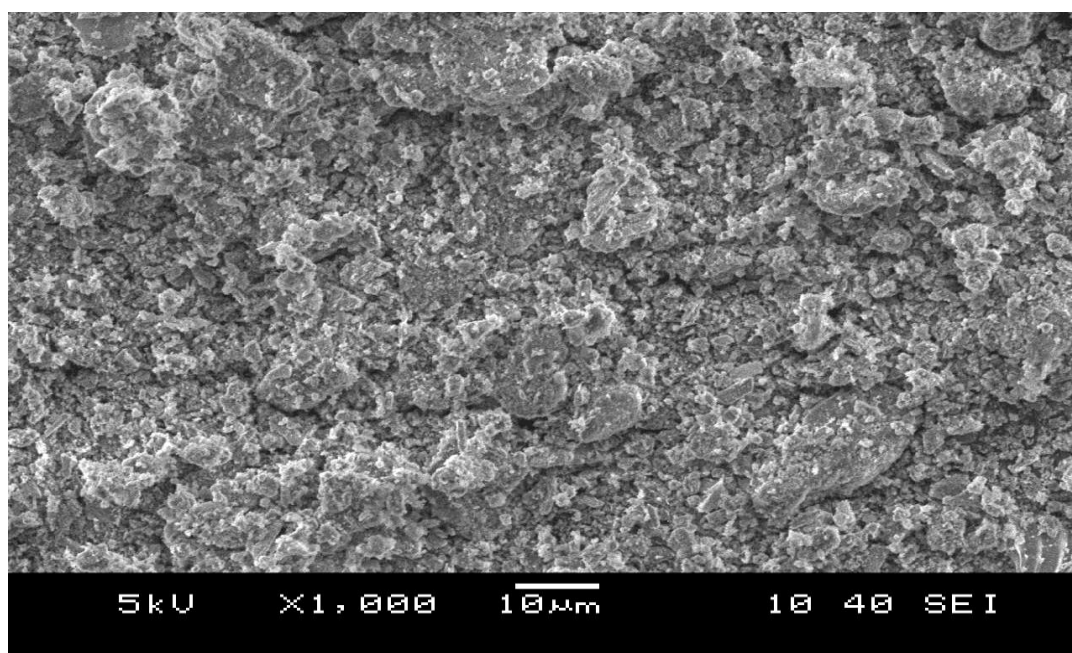


Figure 3.12. SEM Image of Bentonite-Cu(acac)₂

The SEM Images of the Bentonite and Bentonite-based samples (Fig. 3.9-3.12) reflected the main morphology of the Bentonite. After treatment of the Bentonite with APTES and Cu(acac)₂, the morphology was changed to the well-ordered structure and also condensed structural form which may be due to expanded structure of the layers and also the rearrangement of the layers after modification. This

explanation is also in agree with the XRD results which reflected the main structure of Bentonite conserved.

As can be seen from the SEM Images of Siral 80 and Siral-based samples (Fig. 3.9-3.12), the morphology of samples were very different as compared with Bentonite and Bentonite-based samples.

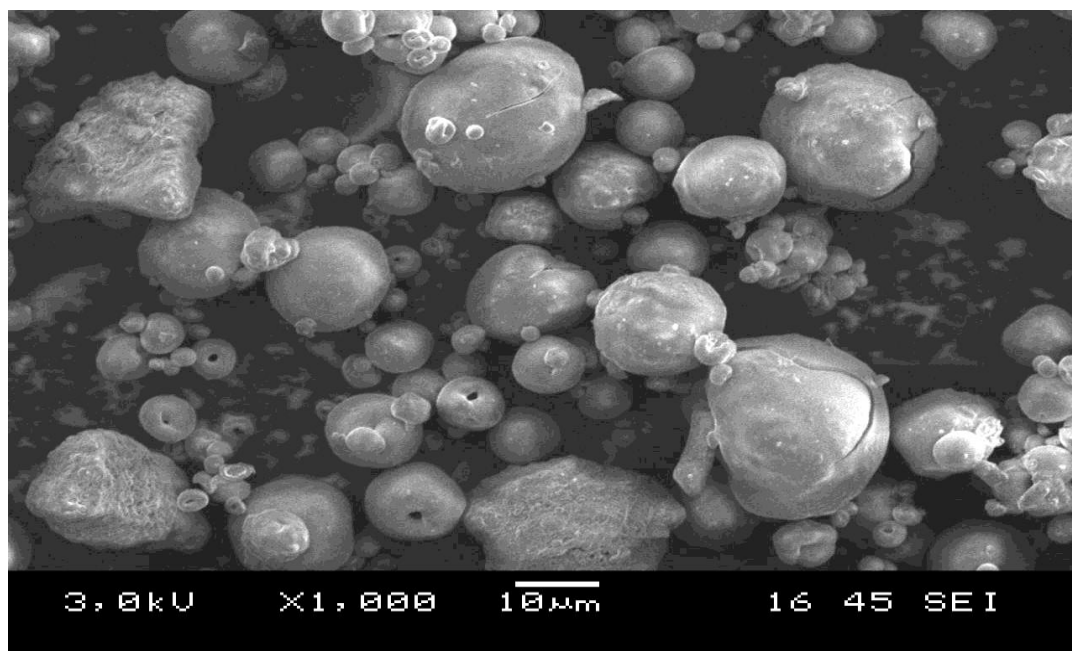


Figure 3.13. SEM Image of Siral 80

The SEM Image of Siral 80 reflected the surface morphology of small, medium and big sized spherical grains. The size of the particles can be calculated from the scale on the image as in the order of 10µm.

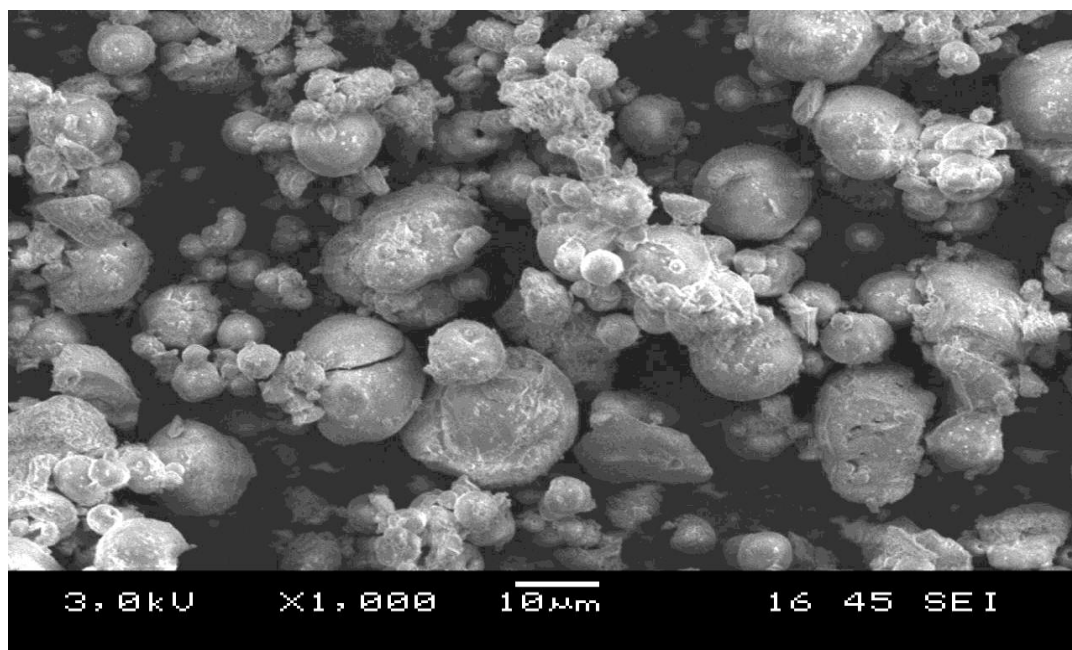


Figure 3.14. SEM Image of Siral 80-APTES

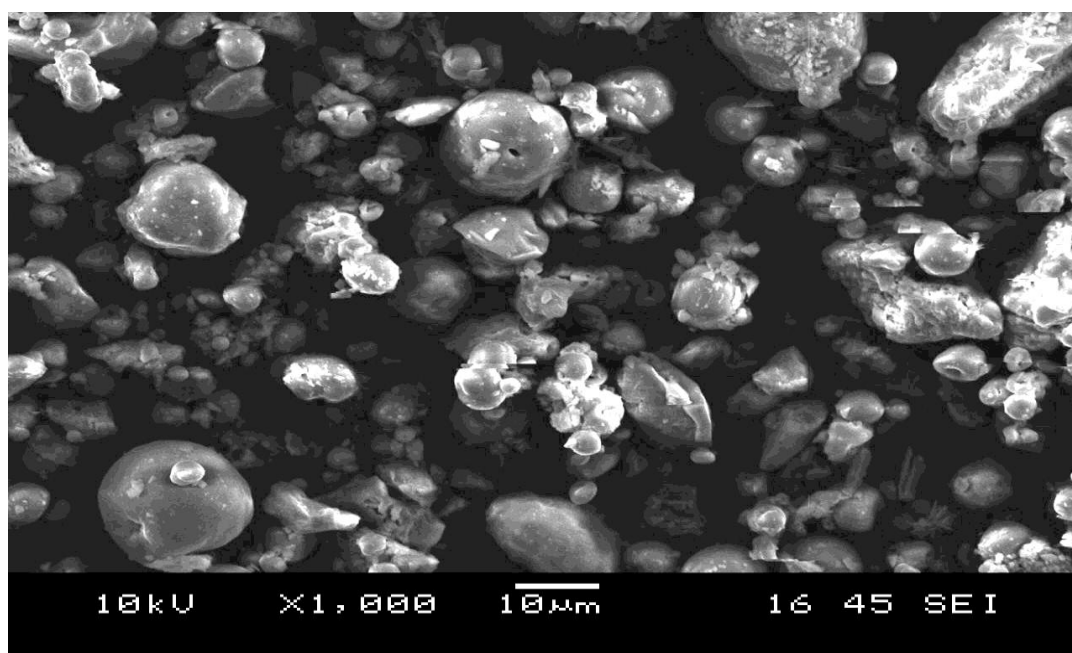


Figure 3.15. SEM Image of Siral 80-APTES-Cu(acac)₂

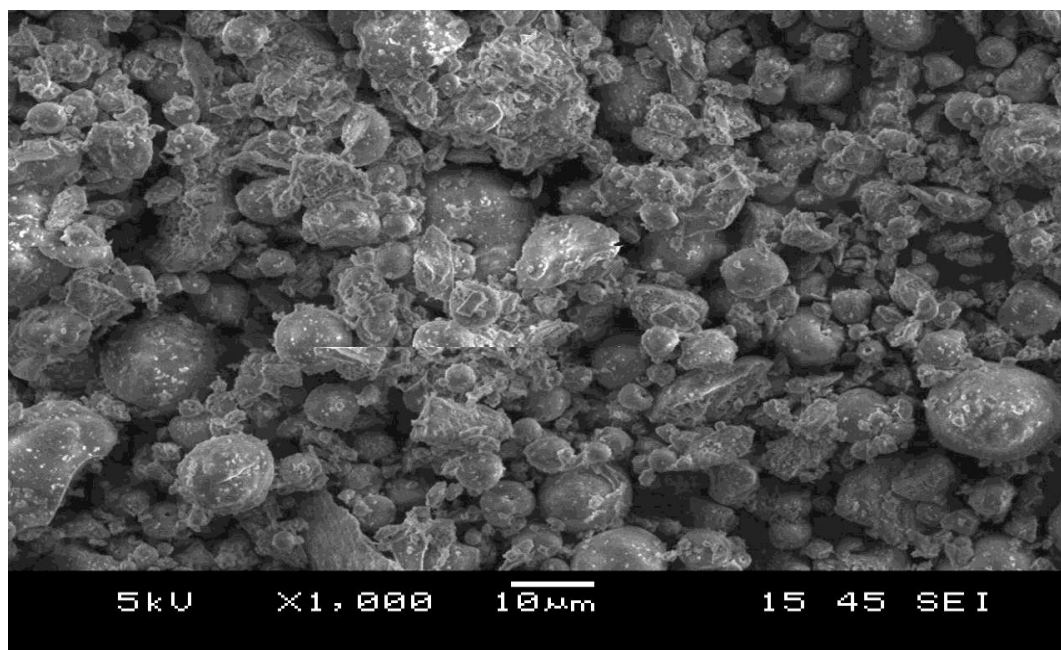


Figure 3.16. SEM Image of Siral 80-Cu(acac)₂

The evaluation of the SEM images of the Siral-based samples reflected the main structure of Siral 80. This means that spherical grains with various sizes. After treatment with APTES and Cu(acac)₂, coagulation of the APTES and Cu(acac)₂ particles onto the surface of the Siral 80 was observed. In the stepwise treatment of them increased the condensity of the particles (sticky small tiny particles) around the spherical grains of Siral 80.

CHAPTER FOUR

DISCUSSION

Copper (II) acetylacetonate has been directly immobilized onto two solid supports, Bentonite and Siral 80 and after their functionalisation with APTES.

The BET specific surface area values of the samples were determined by using the BET method on the N₂ adsorption-desorption isotherms at 77 K which were given as m²/g as in Table 3.4. As indicated in the table, Bentonite had a specific surface area of 65 m²/g while the Bentonite-APTES-Cu(acac)₂ had as 38 m²/g and Bentonite-Cu(acac)₂ had a value of 48 m²/g, respectively. Besides this Siral 80 surface area had a value of 238 m²/g while the Siral 80-APTES-Cu(acac)₂ had as 77 m²/g and for Siral 80-Cu(acac)₂ as 55 m²/g respectively. In contrary to other catalysts surface area values, Siral 80-Cu(acac)₂ had a value smaller than Siral 80-APTES-Cu(acac)₂ so that Siral 80-Cu(acac)₂ holded by the clay surface hydroxyl groups. These results indicated that modification of the Bentonite and Siral 80 surfaces by immobilization procedure decreased the specific surface area due to the fact that coverage of the pores and walls of the pores with APTES or Cu(acac)₂ particles in the preparation period. It may be also because of the attachment of the APTES and copper particles by hydroxyl groups of the edges of Bentonite and surface of Siral 80. On the other hand, for Bentonite, insertion of APTES and Cu(acac)₂ between clay layers are also possible.

According to the AAS analysis results (See page 23), the theoretical amounts of copper in Cu(acac)₂ was calculated as 9180 µg/g. When we compare the copper values on the samples by two methods, the highest copper contents were obtained in the case direct complex immobilization method for Bentonite and Siral 80. On the other hand, firstly APTES modified Bentonite and Siral 80 samples, treatment Cu(acac)₂ resulted a decrease in copper amount as 4550 and 1900 µg/g respectively.

FTIR spectra of the samples are shown Figure 3.1, 3.2, 3.3 and 3.4. The assignments of the bands were also given in the section 3.4 in details and separately. The spectral data reflected in general mainly the FTIR spectra of Bentonite and Siral 80. When the FTIR spectra of the samples compared to the FTIR spectra of Bentonite, Siral 80, APTES and also copper (II) acetylacetonate, the some of the specific bands of APTES and copper (II) acetylacetonate were observed still after modifications. For the FTIR spectra of Bentonite and Bentonite-based samples, the band at around 2927 cm^{-1} , was a new band associated with the $-\text{CH}_2$ stretching vibrations from grafted APTES. The band due to $-\text{NH}_2$ stretching could not be observed, as it is masked by the broad OH stretching band. The band at 1559 cm^{-1} observed in the natural Bentonite (Tabak et al., 2007). The Si–O stretching vibrations were also observed at 668 cm^{-1} . New bands were detected at 659 cm^{-1} , the Si–O which was changed to $-\text{Si-CH}_2\text{-R}$ after APTES treatment of Bentonite. C–N bending vibration was detected at 1383 cm^{-1} . In the range of aliphatic C–H stretching vibrations ($2900\text{--}2700\text{ cm}^{-1}$) no significant changes were observed, even though Cu complex vibrations were expected to occur at the same frequencies in Bentonite-APTES- $[\text{Cu}(\text{acac})_2]$. The band aliphatic C=C- stretching vibrations from $[\text{Cu}(\text{acac})_2]$ at $1500\text{--}1600\text{ cm}^{-1}$ appeared. As well as specific $\text{Cu}(\text{acac})_2$ bands were observed at 1574 cm^{-1} for $-\text{C-C-}$, 1535 cm^{-1} $-\text{C-O-}$ and 1399 cm^{-1} $-\text{CH}_3$, respectively.

For the FTIR spectra of the Siral samples, The band at around 2929 cm^{-1} , there was a new band associated with the $-\text{CH}_2$ stretching vibrations from grafted APTES. The band due to $-\text{NH}_2$ stretching could not be observed, as it was masked by the broad $-\text{OH}$ bending band. C–N bending vibration band was detected at 1220 cm^{-1} . The band at around 1536 cm^{-1} may be attributed to $-\text{C-O-}$ in Siral 80- $[\text{Cu}(\text{acac})_2]$ catalyst sample. The band observed in the band range of $1500\text{--}1600\text{ cm}^{-1}$ was due to the aliphatic C=C- stretching vibrations from $\text{Cu}(\text{acac})_2$.

In general, some small shifts of the bands were also observed due to the immobilization.

According to the XRD analysis, basal spacing values of the samples, Bentonite and Siral 80 were determined and given in Table 3.5 and 3.6. XRD diffractograms were also shown in Figure 3.5 and 3.6. Basal spacing values (d_{001}) for Bentonite, Bentonite-Cu(acac)₂, Bentonite-APTES, and Bentonite-APTES-Cu(acac)₂ showed an increase as 12.67 Å, 15.23 Å, 18.92 Å, 19.28 Å respectively. On the other hand, basal spacing values for Siral 80, Siral 80-Cu(acac)₂, Siral 80-APTES, Siral 80-APTES-Cu(acac)₂ and show a small increase which is not practical as 6.29 Å, 6.51 Å, 6.88 Å, and 6.58 Å. In the X-ray diffractograms for the Siral 80-based materials, no practical change were not observed due to the low crystallite size and the delaminated nature of this material. On the other hand, the diffraction pattern of Bentonite which is expected for this type of material with basal spacing (d_{001}) of 12.67 Å. However, in the case of Bentonite-APTES, in addition to this reflection, a broad peak is also noted at $2\theta=4.67^\circ$ with $d=18.92$ Å, which can be attributed to the expanding of clay due to the intercalation of APTES between the layers. However, the copper (II) complex which was mainly immobilized onto amine-functionalized Bentonite showed an increase between the Bentonite layers. Besides, Cu(acac)₂ is smaller group than APTES-Cu(acac)₂ so Bentonite layer between the openings was increased compared to the size of the Cu(acac)₂.

The thermogravimetric curves for the samples with and without APTES, APTES-Cu(acac)₂ or Cu(acac)₂ were given in Figure 3.7 and 3.8 and Table 3.7 and 3.8. According to the results of TGA/DTG, the total mass losses for Bentonite, Bentonite-APTES, Bentonite-APTES-Cu(acac)₂, and Bentonite-Cu(acac)₂ were found as 23.95%; 20.32%; 24.61%; and 22.5% , respectively. On the other hand, the mass losses for Siral 80, Siral 80-APTES, Siral 80-APTES-Cu(acac)₂ and Siral 80-Cu(acac)₂ were found as 18.98%; 20.07%; 19.37% and 21.01%, respectively. These results indicated that Cu(acac)₂ are added to the structure to be more of ion exchange leads by comparison with the mass losses of Bentonite and Siral 80. As can be seen from Table 3.7 that the mass loss in the first step in Bentonite-APTES-Cu(acac)₂ catalyst was less than Bentonite-APTES and Bentonite which reflects an increase in the thermal stability of Bentonite-APTES-Cu(acac)₂ catalyst. At the same time, similar behavior was also observed in Siral catalysts.

REFERENCES

- Ahenach J., Collar O. & Vansant E.F. (2000). Al-modified porous clay heterostructures with combined micro and mesoporosity. P. Coor, *Studies in Surface Science and Catalysis*, 129.
- Alemdar A., Atıcı O. & Gungor N. (2000). The influence of cationic surfactants on rheological properties of Bentonite–water systems, *Materials Letters*, 43, 57–61.
- Alemdar A. & Gungor N. (2005). The rheological properties and characterization of Bentonite dispersions in the presence of non-ionic polymer PEG, *Journal of Materials Science*, 40, 171– 177.
- Araujo E.M., Melo T.J.A., Santana L.N.L., Neves G.A., Ferreira H.C., Lira H.L., Carvalho L.H., Avila M.M., Pontes M.K.G. & Araujo I.S. (2004). The influence of organo-Bentonite clay on the processing and mechanical properties of nylon 6 and polystyrene composites, *Materials Science and Engineering*, 112, 175–178.
- Bailey S.W. (1980). Summary of recommendations of AIPEA [Association Internationale Pour l'Étude des Argiles] nomenclature committee on clay, *Am Mineral*, 65, 1–7. Available:
http://www.minsocam.org/msa/collectors_corner/arc/nomenclaturecl1.htm.
- Bernstein M., Pairon J-C, Morabia A., Gaudichet A. & Janson X. (1994). Non-fibrous dust load and smoking in dental technicians: a study using bronchoalveolar lavage, *Occup Environ Med*, 51, 23–27.
- Caglar B., Afsin B., Tabak A. & Eren E. (2008), Characterization of the cation-exchanged Bentonites by XRPD, ATR, DTA/TG analyses and BET measurement, *Chemical Engineering Journal*, 7.

- Daniell W., Schubert U., Glöckler R., Meyer A., Noweck K. & Knözinger H. (2000), Enhanced surface acidity in mixed alumina–silicas: a low-temperature FTIR study, *Applied Catalysis A: General*, 196, 247–260.
- Eren E. & Afsin B. (2008), An investigation of Cu(II) adsorption by raw and acid-activated Bentonite: A combined potentiometric, thermodynamic, XRD, IR, DTA study, *Journal of Hazardous Materials*, 151, 682–691.
- Erdem B., Özcan A., Gök Ö. & Özcan A. Safa (2009), Immobilization of 2,2'-dipyridyl onto Bentonite and its adsorption behavior of copper(II) ions, *Journal of Hazardous Materials*, 163, 418–426.
- Hernandez O., SIDS Initial Assessment Report For SIAM 17, Arona, Italy, 11-14 November 2003 Retrieved: June, 2010 from <http://www.inchem.org/documents/sids/sids/919302.pdf>.
- Karapinar N. & Donat R. (2009), Adsorption behaviour of Cu²⁺ and Cd²⁺ onto natural Bentonite, *Desalination* 249, (123–129).
- Katsioti M., Katsiotis N., Rouni G., Bakirtzis D. & Loizidou M. (2008), The effect of Bentonite/cement mortar for the stabilization/solidification of sewage sludge containing heavy metals, *Cement & Concrete Composites*, 30, 1013–1019.
- Lagadic I.L. (2006), Schiff base chelate-functionalized organoclays, *Micropor. Mesopor. Mater.*, 95, 226-233.
- Ma L & Tang J. (2002) Refined kaolin in China. Quality improvements needed to meet future paper demand. *Ind. Miner.*, 415, 66–71.
- Orolinova Z., & Mockovciakova A. (2009), Structural study of Bentonite/iron oxide composites, *Materials Chemistry and Physics*, 114, 956–961.

- Paluszkiewicz C., Holtzer M. & Bobrowski A. (2008), FTIR analysis of Bentonite in moulding sands, *Journal of Molecular Structure*, 880, 109–114.
- Patel H. A., Somani R. S., Bajaj H. C. & JasraRaksh V. (2007), Synthesis and characterization of organic Bentonite using Gujarat and Rajasthan clays, *Current Science*, Vol. 92 No. 7.
- Pereira C., Patrício S. & Silva A. R. (2007), Copper acetylacetonate anchored onto amine-functionalised clays, *Journal of Colloid and Interface Science*, 316, 570–579.
- Pereira C., Silva A. R., Carvalho A. P., Pires J. & Freire C. (2008), Vanadyl acetylacetonate anchored onto amine-functionalised clays and catalytic activity in the epoxidation of geraniol, *Journal of Molecular Catalysis A: Chemical*, 283, 5–14.
- Potter E.V. & Stollerman G.H. (1961) The opsonization of Bentonite particles by gamma-globulin. *J Immunol*, 87, 110–118.
- Rajender V. S. (2002), Clay and clay-supported reagents in organic synthesis, *Tetrahedron report number*, 58, 1235-1255.
- Rieder M., Cavazzini G., D'yakonov Y.S., Frank-Kamenetskii V.A., Gottardi G., Guggenheim S., Koval P.V., Müller G., Neiva A.M.R., Radoslovich E.W., Robert J-L, Sassi F.P., Takeda H. & Weiss Z. (1998), Nomenclature of micas, *Clays Clay Miner*, 46, 586–595.
- Sherenkov I. & Zlatunova D. Retrieved November 2010, from http://echo2.epfl.ch/VICAIRE/mod_3/chapt_1/pictures/fig1_2.jpg.
- Stumm W. (1997) Reactivity at the mineral–water interface: dissolution and inhibition, *Colloids Surf A*, 120, 143–166.

- Tabak A., Afsin B., Caglar B. & Koksall E. (2007), Characterization and pillaring of a Turkish Bentonite (Resadiye), *Journal of Colloid and Interface Science*, 313, 5–11.
- Weber J.B. & Perry P.W. (1965), The influence of temperature and time on the adsorption of paraquat, diquat, 2,4-D and prometone by clays, charcoal, and an anion-exchange resin, *Soil Sci Soc Am Proc*, 29, 678–688.
- Weber J.B. (1970) Adsorption of s-triazines by montmorillonite as a function of pH and molecular structure. *Soil Sci Soc Am Proc*, 34, 401–404.
- Xi Y., Mallavarapu M. & Naidu R. (2009), Preparation, characterization of surfactants modified clay minerals and nitrate adsorption, *Applied Clay*, 5.
- Yurdakoç M., Seki Y., Karahan S., & Yurdakoç K. (2005), Kinetic and thermodynamic studies of boron removal by Siral 5, Siral 40, and Siral 80, *Journal of Colloid and Interface Science*, 286, 440–446.
- Zhansheng W., Chun L., Xifang S., Xiaolin U. & Jine L. (2006), Characterization, Acid Activation and Bleaching Performance of Bentonite from Xinjiang, *Chinese J. Chem. Eng.*, 14(2), 253-258.
- Zhou C., Li X., Ge Z., Li Q. & Tong D. (2004), Synthesis and acid catalysis of nanoporous silica/alumina-clay composites, *Catalysis Today*, 93–95, 607–613.
- Zhu L., Tian S., Zhu J. & Shi Y. (2007), Silylated pillared clay (SPILC): A novel Bentonite-based inorgano–organo composite sorbent synthesized by integration of pillaring and silylation, *Journal of Colloid and Interface Science*, 315, 191–199.